Processes **2014**, *2*, 466-493; doi:10.3390/pr2020466

OPEN ACCESS

processes

ISSN 2227-9717

www.mdpi.com/journal/processes

Review

Microreactors for Gold Nanoparticles Synthesis: From Faraday to Flow

Md. Taifur Rahman and Evgeny V. Rebrov *

School of Chemistry and Chemical Engineering, Queen's University Belfast, Stranmillis Road, Belfast BT9 5AG, UK; E-Mail: t.rahman@qub.ac.uk

* Author to whom correspondence should be addressed; E-Mail: e.rebrov@qub.ac.uk; Tel.: +44-028-9097-4627.

Received: 15 January 2014; in revised form: 15 March 2014 / Accepted: 1 April 2014 / Published: 5 June 2014

Abstract: The seminal work of Michael Faraday in 1850s transmuted the "Alchemy of gold" into a fascinating scientific endeavor over the millennia, particularly in the past half century. Gold nanoparticles (GNPs) arguably hold the central position of nanosciences due to their intriguing size-and-shape dependent physicochemical properties, non-toxicity, and ease of functionalization and potential for wide range of applications. The core chemistry involved in the syntheses is essentially not very different from what Michael Faraday resorted to: transforming ions into metallic gold using mild reducing agents. However, the process of such reduction and outcome (shapes and sizes) are intricately dependent on basic operational parameters such as sequence of addition and efficiency of mixing of the reagents. Hence, irreproducibility in synthesis and maintaining batch-to-batch quality are major obstacles in this seemingly straightforward process, which poses challenges in scaling-up. Microreactors, by the virtue of excellent control over reagent mixing in space and time within narrow channel networks, opened a new horizon of possibilities to tackle such problems to produce GNPs in more reliable, reproducible and scalable ways. In this review, we will delineate the state-of-the-art of GNPs synthesis using microreactors and will discuss in length how such "flask-to-chip" paradigm shift may revolutionize the very concept of nanosyntheses.

Keywords: gold nanoparticles; microfluidics; core-shell; nanorods; scale-up

---

1. Introduction: Gold Nanomaterials—Syntheses and Applications

Gold is one of the most important elements in the human civilization. In early human societies, gold was a symbol of power and wealth, and was used as ornaments for both living and the dead. Gold has been, ever since the very dawn of commerce, a reliable and universal means of financial transactions and reserve. Hence, the desire and dream of "transmuting anything into gold" paved the way for alchemy, which is the predecessor of modern Chemistry. Rather unknowingly, non-bulk form of gold had also been a part of humanity from the time of antiquity. Colloidal gold dispersed in glass or ceramics produce hues of red or green, which were used to decorate and color Roman cage-cups, or diatretum. One famous example is the Lycurgus cup, dating from the 4th century A.D., made from nanogold-infested glass, now preserved in the British Museum in London.

Although widely used throughout the history for decorative purposes and as medicines [1,2], the nature of colloidal gold was investigated only sporadically [3]: In 1676, a German chemist, Johann Kunckels, inferred that non-bulk gold exists in infinitesimal state that is not visible to human eyes. It was Michael Faraday who pioneered the first systematic synthesis of gold nanoparticles using phosphorous-based reducing agents. He is widely credited for insightful and for the "first" scientific discussion on size dependent optical properties and their coagulation behavior of colloidal gold [4].

Rapid growth in interests about colloidal gold was sparked by the availability of electron microscopes that enabled direct visualization of the nanoparticles [5,6]. Over the past two decades, tremendous effort was dedicated to synthesize and optimize a wide class of GNPs possessing a broad spectrum of geometry, size, chemistry and functionality. This paved the way for applications of GNPs in heterogeneous catalysis, bio-imaging, medicines, optics, analytical sciences, sensing, *etc*. [7–17]. Because of widespread applications of GNPs in different branches of sciences and technologies, need for establishing reliable supply chains for such materials is becoming ever more important, hence the involved chemical processes are of utmost importance.

2. Mechanism and Challenges in Metallic Nanoparticles Synthesis

Interestingly, typical GNPs synthesis protocols adapted by most leading research groups are as simple as Michael Faraday's experiments in the 1850s: reduction of gold ions (usually Au(III) salts) in a solution using reducing agents. However straightforward the synthesis may appear, the underlying mechanisms of the elementary processes involved in the formation of metallic colloids from homogeneous mixture of ionic precursors (gold ions and reducing molecules/ions) are rather complex. Formation of such materials from homogeneous state involves several interconnected and interrelated steps: (1) species undergoing reduction leading to supersaturation for metallic atoms in the reaction volume; (2) formation of nuclei from these insoluble metal atoms either by diffusive growth or aggregation; and (3) growth of the nuclei into the final nanostructure by diffusion of atom/ions to the nuclei surface and on-surface deposition/auto-catalytic reduction via electron transfer from the reducing agent [18,19].

The intrinsic kinetics of these elementary steps rather than the thermodynamics defines the outcome of the reactions. Mixing of gold ions with reducing agent is of vital importance, because any inhomogeneity in the mixing will generate concentration gradients in the reaction volume. As such,

inhomogeneity would cause random nucleation producing nuclei with variable sizes that would grow into final nanoparticles having poor size distribution. In addition, if the nucleation step is not complete before the growth starts, then there will be a competition for gold ions between two parallel processes: new nucleation and growth of the present nuclei; which is responsible for polydispersity in size and shape. Even if the nucleation is performed properly, homogeneous supply of gold ions to the surface is required for the controlled diffusive growth. Hence, nucleation and growth steps should be separated in time to facilitate monodisperse GNP production. Such a scenario is not often achievable in reproducible manner in conventional stirred reactors (typically flasks). Usually characteristic mixing time is relatively long as compared to nucleation time in conventional reactors. This results in variation of local temperature, pH or reactant concentrations that contribute to polydispersity and poor batch-to-batch reproducibility. All these factors underscore the necessity for an alternative platform for synthesis of these nanomaterials, which is not only reliable and reproducible but also robust enough for scalable production of various types of gold nanoparticles.

3. Scope of the Review

Over the past decade microreaction technology evolved as a miniaturized version of flow reactors [20–22]. Unlike conventional continuous stirred tank reactors (CSTR), mixing between two or more reacting fluids takes place within tens of micrometers length. Hence, complete mixing between reactants occurs in micro-to-millisecond time scale. Due to the small dimensions of the mixing and reaction region, unprecedented control over mass-and-heat transport and reaction time is possible. Initial success of implementing microreaction technology in organic synthesis prompted several groups to resort to microfluidic reactors to circumvent challenges (vide infra) associated with nanomaterials synthesis. There are several recent reviews covering the use of microfluidic reactors for the synthesis of nanoparticles of different kinds [23–26]. Here an overview is provided on how flow synthesis methods leveraged for a wide variety of GNPs possessing superior quality compared to the products obtained from batch processes. Scaling up approaches will also be discussed.

4. Synthesis of Colloidal Gold Nanoparticles in Microreactors

Wagner *et al*. were the first to report synthesis of gold nanoparticles in a microreactor [27]. They used a microfluidic chip fabricated from Pyrex glass by wet etching method. The chip consisted of two micromixers and a residence time unit (Figure 1). In the first micromixer, a solution of ascorbic acid, acting as a reducing agent, was mixed with preformed gold seeds of 12 nm in diameter. This mixture was guided through a serpentine channel to complete mixing. Then, reduction of the gold ions onto the good seeds started in the second micromixer with a volume of 2.3 μL where a solution of chloroauric acid was added to the flow to keep the total flow rate in the range of 5–50 μL/min. The reaction mixture was collected from the reactor outlet via a PTFE tube and analyzed by spectroscopic and microscopic methods.

The channel walls were negatively charged at the pH of 10, used in all experiments. When citrate ions were used as capping agent, the surface of gold nanoparticles was also negatively charged. Therefore electrostatic repulsion prevented seed deposition onto the inner channel walls. However, when the seeds were grown in the presence of ascorbic acid, significant gold deposition on the walls

was observed. This undesirable deposition was reduced by increasing the seed to gold ion ratio in the solution. At the 1:1 molar ratio, gold particles with a size of 24 nm were obtained, albeit with poor monodispersity. The size was further controlled by varying the respective flow rates of the reactants and/or the reducing agents.

Figure 1. Microfluidic device for GNP synthesis. Adapted from Ref. [27] (with permission from Elsevier Ltd.

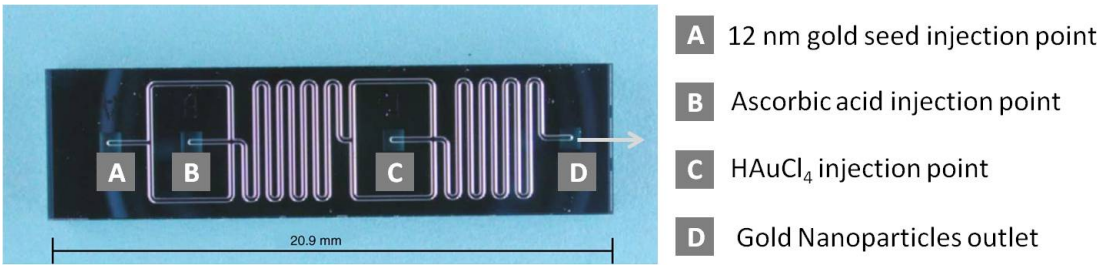

In the absence of seeds in the synthesis with ascorbic acid, both high pH of the reaction mixture and highly hydrophobic surface of the inner reactor walls prevented the nanoparticle deposition onto the inner walls of a pyrex/silicone microreactor [28]. A principle of split-and-recombine mixing was utilized in this microreactor. The hydrophobic surface was created by modification with perfluorosilane and polyvinylpyrrolidone (PVP) was used as capping agent. As the flow rate increased, the mean diameter of the gold nanoparticles decreased, while the total number of nanoparticles increased. It has been shown that there exists a range of flow rates, where axial dispersion effects can be neglected leading to improved control over mixing. The obtained gold nanoparticles showed better distribution, which was twice as narrow in comparison to those obtained in the conventional reactor and in the microreactor with a substantial degree of backmixing observed at low flow rates. In a follow up work, controlled accumulation of the discrete nanoparticles into larger clusters of micrometer size was demonstrated in the channels of 180 × 200 μm^2 made in a glass chip [29]. In this reactor, a solution of reducing agents (ascorbic acid and iron(II) sulfate) was mixed with polyvinyl alcohol in the first mixer. Then, a sodium metasilicate solution was introduced in the second mixer and gold ions were injected in the third mixer. Reduction of gold ions into colloidal gold in the presence of polymer and electrolytes facilitated the clustering of gold nanoparticles into larger clusters. Small GNPs with a diameter of 3–5 nm were obtained when sodium borohydride was used as reducing agent [30]. The size can further be fine-tuned by controlling the concentration (via dilution by introducing diluents water stream) of the gold ions and borohydride. Thus, the authors were able to control the cluster size between 3 nm up to micrometer size by varying the respective flow rates and concentration.

Ultra-small gold clusters with a diameter of 1 nm are an important class of gold nanomaterials with regards to their high catalytic activity in many organic reactions [31]. Synthesis of such gold clusters is a difficult task in conventional stirred reactors due to pure control of mixing. Deviations of the local concentration of reactants, particularly strong reducing agents like sodium borohydride, influence the kinetics of the cluster formation and are detrimental to the size distribution. Tsunoyama *et al*. presented a microfluidic method to produce ultra-small PVP-stabilized gold nanoparticles using a SIMM-V2 micromixer (IMM, Figure 2A) [32]. In this micromixer, the total flow of $HAuCl_4$ gold precursor, PVP and an aqueous solution of sodium borohydride was split in a multitude of parallel

substreams with a thickness below 100 μm. This reduced characteristic diffusion time from several minutes to a few seconds. Moreover, it was speculated that microbubbles, which were formed due to the decomposition of borohydride, assisted in breaking the lamellar structure into smaller fragments, further accelerating the mass-transport. Sub 2 nm gold nanoparticles were produced with a monodispersity of 14% from a 10 mM Au precursor solution at a relatively low PVP:Au molar ratio of 40:1 Figure 2B). It should be noted that larger and polydisperse PVP-protected Au clusters were produced in a conventional reactor, when similar concentrations of reactants were used (Figure 2C). The activity of Au clusters in oxidation of 4-hydroxybenzyl alcohol was 50% greater than that with Au clusters produced by classical batch protocol demonstrating the advantages of monodispersed Au nanoparticles in structure sensitive reactions.

Figure 2. (**A**) Multilamination and mixing of gold precursors (Au ions and PVP) with reducing agent (sodium borohydride and PVP); (**B**,**C**) TEM photographs of produced GNPs with size distribution (insets) for microfluidic and batch processes, respectively. Adapted from Ref. [32] (with permission from American Chemical Society).

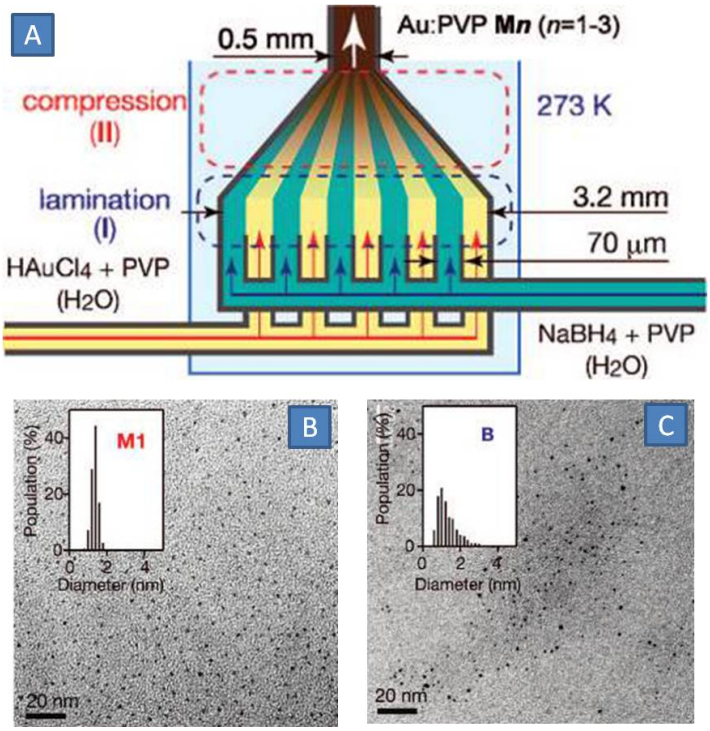

The SIMM-V2 micromixer in combination with a microreactor was employed to examine the dependence of the particles size on the reactant flow rates [33]. The authors used $HAuCl_4$ as gold source, while ascorbic acid and PVP were used as reducing agent and surfactant, respectively. They obtained a set of GNPs with different sizes in the range from 1.7 to 33 nm by varying the flow rate from 7.5 to 0.1 mL/min. The characteristic half time of ascorbic acid mediated reduction of gold ions was found to be 31 ms. Still, this is much shorter as compared to the characteristic diffusion time of at least several seconds. As the diffusion time approaches the characteristic reaction time, it enables to decouple the nucleation and growth steps, which in turn provides better degree of control over the particle size via variation of the residence time. The authors did not observe deposition of on the inner metal walls of the micromixer at high flow rates.

5. Effect of pH

Ishizaka *et al*. adjusted the pH of a gold precursor solution with addition of an aqueous sodium hydroxide solution in a Teflon mixer connected to a capillary [34]. This solution was then mixed with glucose acting as reducing agent. As the hydroxide flow rate decreased, the pH of the resulting solution decreased too yielding non-spherical GNPs as detected by a blue shift in the light absorption (Figure 3). At a pH of 6.9, star-like GNPs were obtained solely in the microreactor, while in their batch system this morphology could not be obtained at the same reaction conditions.

Figure 3. Upper panel: Microfluidic pH Control of Gold solution with NaOH and then online reduction with glucose. Lower panel: GNP samples of wide UV absorption characteristics (depending on shape); TEM photograph of star-like GNP (while line at the bottom left of TEM photo corresponds to scale bar, in addition to the bottom right side, unaltered from the original image). Adapted from Ref. [34] (with permission from Elsevier Ltd.).

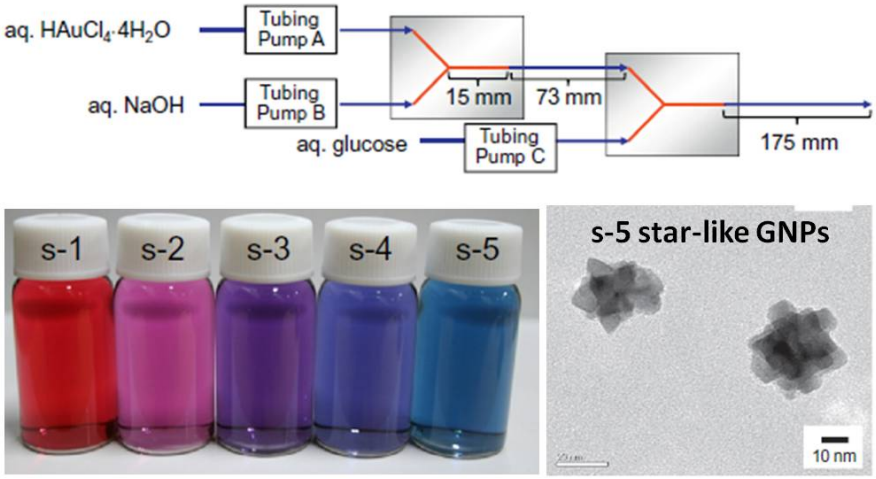

It is known that the reducing potential of ascorbic acid depends on the pH of the solution. At pH below 4.1, ascorbic acid exists in the protonated form, $AscH_2$. As the pH increases, it transforms into ascorbate, $AscH^-$, while at pH above 11.6 it is completely deprotonated to form, Asc^{2-}. Such speciation of ascorbic acid at different pH alters its reducing power. The control of the initial pH of the ascorbic acid solution increased the isolation of spherical GNPs, with high monodispersity [35]. Au nanoparticles with average diameter of 18, 10 and 7 nm, with narrow relative polydispersity indices of 0.4, 0.3 and 0.2 were obtained from a $HAuCl_4$/ascorbic acid mixture at a pH of 10.2, 10.7 and 11.1, other parameters being the same. The initial pH was adjusted with a sodium hydroxide solution. A microfluidic mixer was operated at Reynolds number of 2000, enabling intense mixing between ascorbic acid and gold precursors.

6. Transient Operation

A pulsed dosage of 0.5 μL of a 1 mM Au(III) solution (every 2 s) to a continuous flow of a 1.5 mM sodium borohydride solution was proposed by Pedro *et al*. [36]. The two solutions were mixed in a flow-focusing T-junction connected to a three-dimensional serpentine channel network

(Figure 4A,B). This enabled controlled and homogeneous formation of the gold seed/nuclei due to the creation of supersaturated zones in each dosed volume of gold ions. The entire microreactor was made by low-temperature co-fired ceramic technology (LTCC). Highly reproducible 2.7 nm GNPs with high monodispersity were obtained in at least 10 consecutive runs (Figure 4C,D).

Figure 4. (**A**) Microfluidic device made by low-temperature co-fired ceramic technology LTCC; (**B**) Micromixer and 3-D serpentine residence time unit enabling efficient mixing; (**C**) Reproducibility between several runs of experiment; (**D**) TEM photograph: Size-distribution of GNPs in the form of histogram is provided in the inset; mean average diameter is 2.7 nm for the Mercaptoundecanoic acid MUA modified gold nanoparticles. Adapted from Ref. [36] (with permission from IOP Publishing Ltd.).

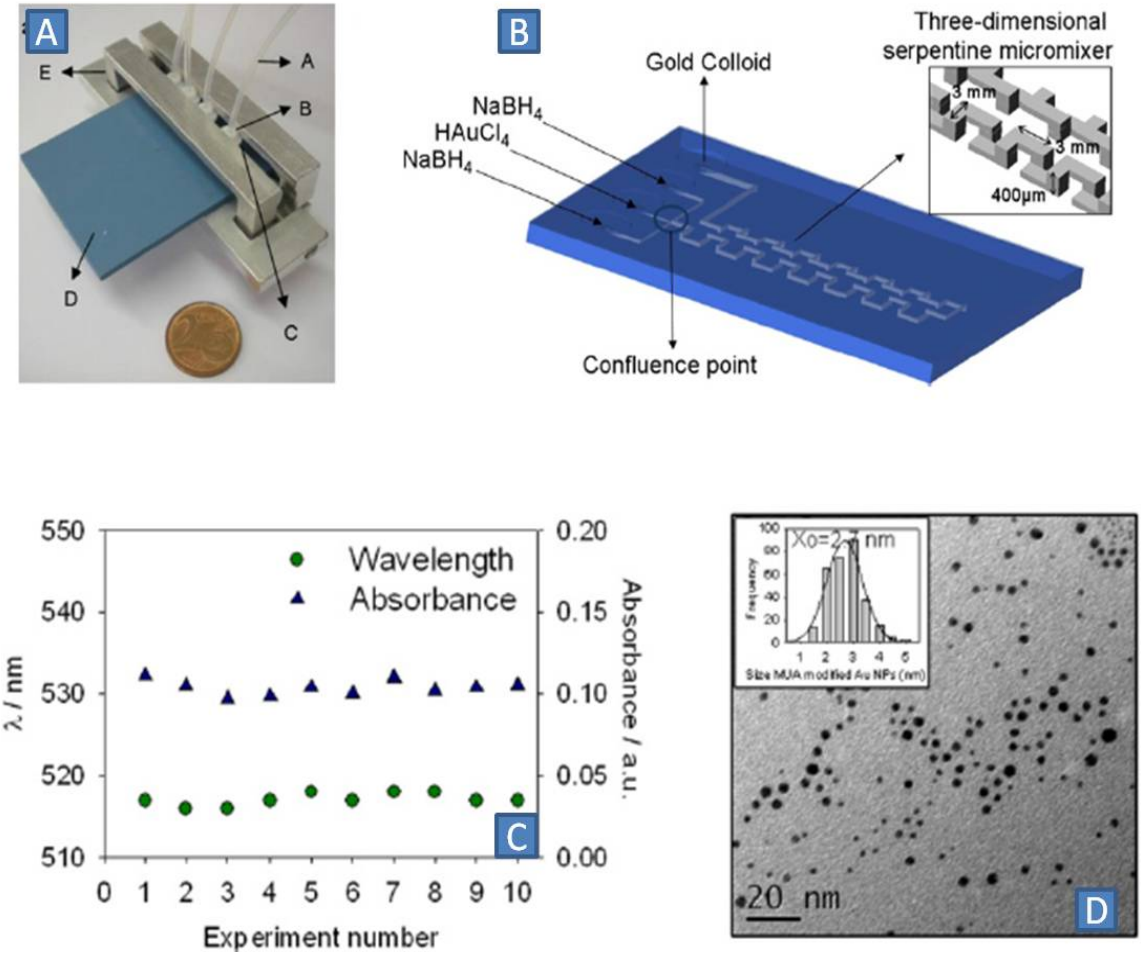

Ultra-small Au nanoparticles can also be obtained by rapid heating and quench in a microreactor system [37]. In this method, the Au ions are reduced with a sodium citrate solution at elevated temperature, just below the boiling point of the solvent, yielding a multitude of nuclei that needs to be immediately cooled to arrest further growth. A T-mixer was connected to a 1.5 m fused silica capillary with a diameter of 200 µm maintained at 100 °C (Figure 5A). The outlet flow was rapidly cooled to quench the reaction. With a residence time of 35 s, gold nanoparticles with an average diameter of 2 nm were produced at a citrate: Au molar ratio of 3.5 (Au 5.4 mM), while the synthesis in batch gave a polydispersed mixture of gold nanoparticles under similar reaction conditions. Different particle sizes in the range of 1.5–3.0 nm were obtained by varying the residence time in the

microreactor (Figure 5B). Thus, fast heating enabled to obtain ultra-small GNPs even with classical synthesis methods.

Figure 5. (**A**) T-mixer and Fused Silica capillary microreactor; (**B**) GNP Size variation and size distribution by tuning residence time. Adapted from Ref. [37] (with permission from Royal Society of Chemistry).

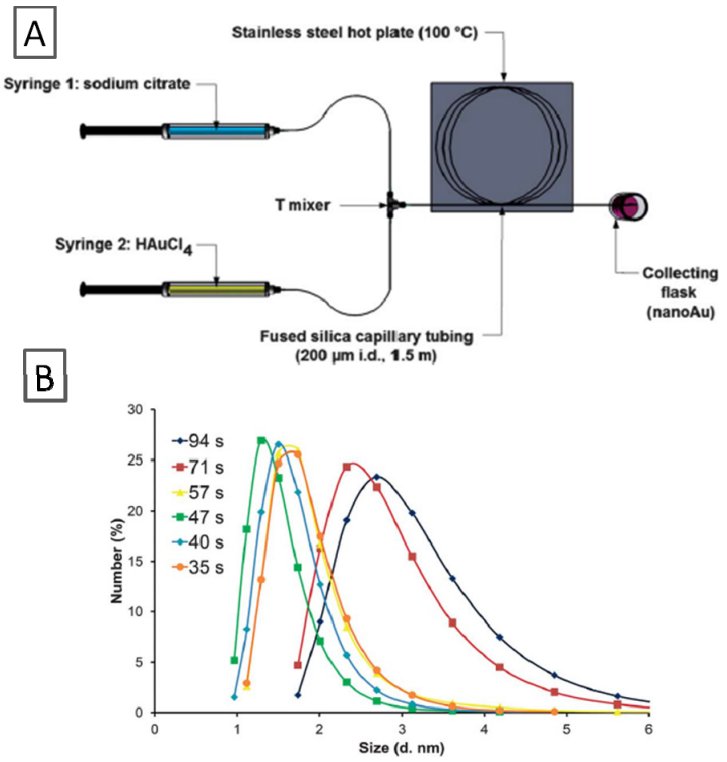

7. Surfactant Stabilized Gold Nanoparticles

While many reports are devoted towards preparing water-dispersible GNPs colloids in microfluidic reactors, less attention was given to organically-capped hydrophobic gold nanoparticles which are also an important class of GNPs. Sugie *et al*. reported reduction of $HAuCl_4$ in tetrahydrofuran (THF) solvent inside a Y-mixer/PTFE microreactor assembly maintained at constant temperature (25–60 °C) using organosilanes (RSiH) as reducing agents and alkyl thiol (RSH) as capping agent [38]. The effect of the residence time and temperatures was studied. As the residence time increased from 12 to 94 min, the size of the GNPs increased from 4.3 to 8.7 nm. The nature of the reducing agent did not alter the size of GNPs when the flow rate and temperature were kept constant. A benchmark experiment in the batch mode at 60 °C produced insoluble precipitates manifesting uncontrolled growth.

8. Development of Time Resolved Analysis Techniques to Monitor Reaction Kinetics

It is generally considered that the kinetics of nucleation and growth is coupled and in most cases extremely fast. Hence, monitoring the nucleation and growth processes in real-time is even more challenging than harnessing such processes to produce GNPs in size/shape-controlled manner. Krishna *et al*. presented a fluidic method to examine the real-time nucleation and growth kinetics by employing on-line X-ray absorption spectroscopy (XAS) [39]. This method provides kinetic profiles of

the nucleation and growth of gold nanoparticles on the channel surface. To obtain time resolved information about the growth of gold nanoparticles, an X-ray beam with a size of 50 × 50 μm^2 was directed via a micromixer where a $HAuCl_4$ solution was contacted with a meso-2,3-dimercapto succinic acid solution at relatively low Re numbers (Figure 6). In such conditions, a gold-thiol species was formed and deposited onto the inner channel surface. Then, a sodium borohydride solution was fed through the microchannel to reduce the Au-Thiol species o colloidal GNPs. The latter step was monitored with XAS at 5 ms intervals at different locations of the channel.

Figure 6. Upper panel: Microfluidic device for in-situ monitoring of GNP growth kinetics with an X-Ray probe, Lower panel: time-resolved deposition of gold nanoparticles and aggregation along the microfluidic channel at different positions. Adapted from Ref. [39] (with permission from American Chemical Society).

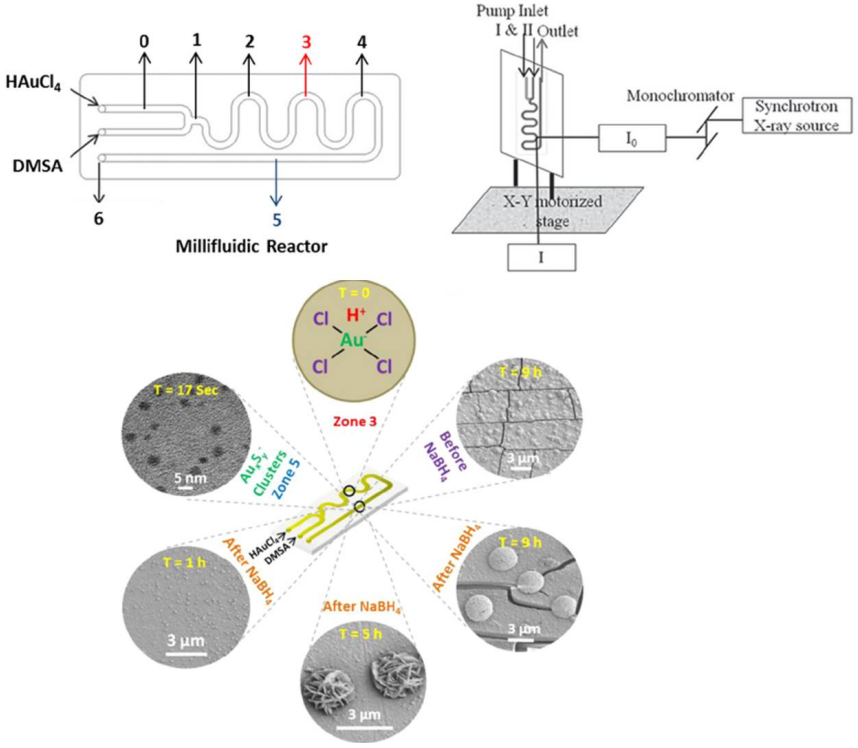

9. Synthesis of Composite GNPs

Au-Metal Composites

During the last fifteen years, core-shell nanoparticles have been intensively studied for their potential to have specific optical, electronic, magnetic and catalytic properties. Several research groups have employed microfluidic reactors for the synthesis of complex gold nanoparticles, such as Au-Ag (gold-silver) composites, core-shell (Au/Ag or Au/Silica), gold nanorods, *etc*. [8,40–47]. Due their tunable optical and chemical properties, these materials hold large promises in optics, analytical and biosciences as imaging and therapeutic agents. The choice of noble-metal (Au) core is motivated by the strong optical responses resulting from the well-known surface plasmon resonance, thus allowing construction of efficient probes for surface enhanced Raman scattering. However, those properties require suppression by use of surface encapsulation of the tendency of the nanoparticles to aggregate.

Moreover, the use of dielectric materials such as metal oxides for the shell coating can allow further tuning of those properties. As a consequence, optimization of this tailoring requires a precise control of the chemical composition, the structure and dimensions of the shells. Although such chemically and structurally delicate nano-motifs can be synthesized in flask reactors, however reliable and scalable means to fabricate such materials are highly challenging. Hence, microreactors are envisaged as a robust means to produce such materials in a reliable and scalable fashion.

It should be noted that the rate of the gold reduction step is much higher than that of silver reduction, therefore it is of importance the presence of the silver ions in the vicinity of the gold seeds in order to make core-shell particles. The microfluidic synthesis of Au-Ag core-shell nanoparticles was realized in a Statmix 7 (IPHT Jena) glass/Si/glass split-and-recombine microreactor to ensure multilamination of fluid segments for better mixing via rapid interdiffusion between adjacent laminar layers (Figure 7) [48]. In the first micromixer, an Au(III) aqueous solution was mixed with ascorbic acid to generate gold nuclei. These nuclei act as seeds/core to catalyze the growth of the silver shell onto the gold core once a stream of silver nitrate solution was introduced in the second micrometer. At a low flow rate of 25 μL/min, the rate of diffusion of ascorbic acid into silver-rich laminar layers was relatively slow. As a result, only gold colloids were formed. As the flow rate increased towards the 42–58 μL/min range, proper multi-stacking of lamellas containing Au-ascorbic acid and the Ag salt was realized. This enhanced diffusion of the silver ions to the gold seeds yielding predominantly the Au-Ag nanoparticles. In the intermediate flow regime (42–50 μL/min), both Au-Ag and Au particles were formed. This work demonstrated the importance of mixing and precise control of the reaction time for the synthesis of complex composite materials of desired/tunable chemical composition.

Figure 7. Upper panel: Schematic of Au-Ag core-shell synthesis in microreactor and possible products. Lower panel: Multilamination and mixing efficiency at different flow rates (**A**: typical flow rate 42–58 μL/min, while **B**: 25 μL/min). Adapted from Ref. [48] (with permission from Wiley-VCH).

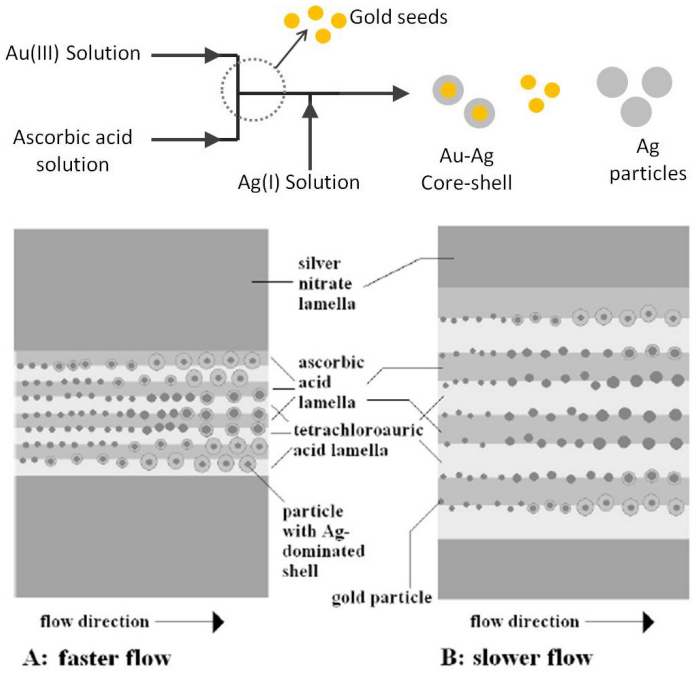

Au-Ag alloy nanocomposites were prepared in a PTFE capillary microreactor with a diameter of 750 μm in a single step (Figure 8) [49]. A preformed solution of silver nitrate, gold chloride, oleylamine and octadecene (Au^{3+}/Ag^{+} = 20) was fed to the microreactor maintained at 140 °C. At this temperature, fast nucleation of gold into the primary core materials was completed prior to thermally assisted diffusion-reduction of Ag inside the Au cores. As the residence time increased from 30 to 320 s, more silver ions diffused towards the gold seeds. As a result, the silver content in the Au-Ag alloy increased commensurately. Highly monodisperse and composition-defined Au-Ag alloy particles with an average diameter of 2.7 nm were produced at a residence time of 3 min. Similar reaction conditions in a batch reactor required longer reaction time and produced Au-Ag nanoparticles with large size distribution.

Figure 8. Schematics of mechanism for Au-Ag alloy synthesis. Change of product composition (colloidal Ag or Au and Au-Ag ally) with residence time inside the microreactor (variation of plasmonic absorption with residence time is shown in the UV-Vis trace of (a)). Adapted from Ref. [49] (with permission from Elsevier Ltd.).

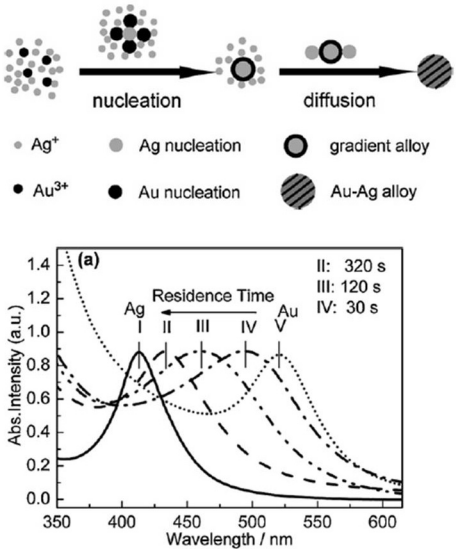

10. Au-Metal Oxide Composites

A uniform gold shell onto dielectric cores such as silica particles exhibits much more pronounced plasmonic properties, which can be utilized in a number of optical and biological applications [41,45]. Such materials sparked intense interests in fundamental and applied research [43]. The thickness of the Au shell and the extent of Au coverage on the silica core dramatically affects the resulting plasmonic behavior. Several groups developed chemical methods to achieve such variation through controlling the reactions. The basic chemistry to form SiO_2@Au nanomaterials involves several steps (Figure 9). It starts with the formation of silica nanoparticles by the Stöber method [50], followed by the functionalization of silica surface with amine containing silane species. The surface becomes positively charged, allowing adsorption of preformed gold seeds. In the last step, the reduction of exogenously added gold ions onto these seeds occurs to form a complete gold shell onto the silica core. Recently, the SiO_2@Au nanomaterials were produced in a Teflon millireactor with a diameter of 1.3 mm by Gomez *et al*. [51]. The amino-functionalized silica particles were obtained by reaction

between an ethanol solution of silica precursor (tetraethyl orthosilicate and 3-aminopropyltriethoxy silane) with an ammonia solution in the flow reactor at 40 °C with a residence time of 30 min. After off-line separation, it was observed a rather big distribution in particle size due to laminar flow and large variation in residence time in the microreactor operated in the laminar regime. In the second step, another microreactor was employed to attach gold seeds (2–4 nm) onto the silica particles. The obtained Au-seeded silica colloids were further treated with a gold salt solution in the presence of formaldehyde as reducing agent. The authors noticed poor attachment of the gold seeds onto the amino-silica cores. As a result, substantial amount of free colloidal gold apart from gold-silica core-shell materials was also observed in the final product, which would require additional purification step. This observation manifests in the necessity of a cleaner process for such materials synthesis, which is often accompanied by undesired side-reactions (here the free colloidal gold formation).

Figure 9. (**a**) Chemical steps for silica particles synthesis, amino functionalization, seeding with Au and the Au shell formation by chemical reduction of gold; (**b**) Microfluidic setup for core-shell synthesis; (**c**) Interdigitated micromixer for mixing of reagents for core-shell synthesis. Adapted from Ref. [51] (with permission from Royal Society of Chemistry).

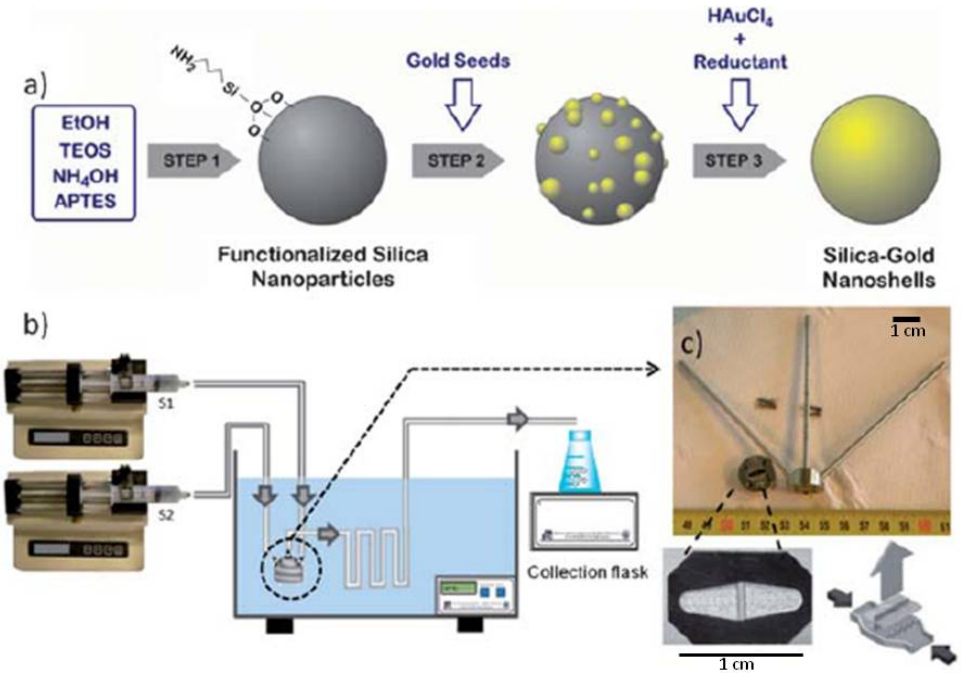

11. Au Nanorods

Gold nanorods (GNRs) is another class of gold nanoparticles, which show surface plasmon behavior [8]. In particular, they can support a longitudinal surface plasmon, which results in suspensions of them having a strong extinction peak in the upper visible or near-infrared parts of the spectrum. The position of this peak can be readily tuned by controlling the shape of the rods. In addition, the surface of the nanorods can be functionalized by a very wide variety of molecules. This has led to interest in their use as selective biomarkers in biodiagnostics or for selective targeting in photothermal therapeutics [46,47,52,53]. Typical gold nanorods are 30–50 nm long and 5–10 nm wide. The plasmon of nanorods splits into two modes of surface electron oscillation: (1) along the long axis,

longitudinal (light absorption beyond 600 nm up to near infrared region) and (2) along the short axis which is typically in the range of spherical gold nanoparticles *i.e.*, 520–530 nm). Longitudinal plasmon can be tuned by controlling the anisotropic growth of gold seeds along the longer axis.

Typically, chemistry of GNRs formation involves templated growth of small gold seeds (1–3 nm) with a growth solution: a mixture of gold salt, ascorbic acid reductant, templating agent CTAB and a small amount of silver nitrate in water. Boleininger *et al*. reported the first GNRs synthesis in a PVC microreactor connected to a three-way valve and a 7-port manifold (Upchurch Scientific) [52]. The authors were able to produce GNRs with different aspect ratio by changing the ratio between the preformed gold seeds solution and the growth solution. In-situ monitoring of the GNRs formation was performed with an optical probe in the downstream part of the microreactor. The effect of the reaction temperature and reactant concentrations was systematically studied. Since preformed seeds for GNRs are not stable over a period of several hours, only freshly prepared seeds can serve as reliable core materials for their growth into monodisperse GNRs. In this way, Bullen *et al*. modified this synthesis by employing a sequentially rotating tube processor (RTP) connected to a microfluidic chip to perform sequential operations of seed formation and growth of seeds into GNRs (Figure 10) [53]. A stable continuous operation for 19 days was demonstrated, which would be hampered had they used presynthesized seeds. Spectral data for all the samples collected over 19 days of operation demonstrate the robustness of the system to produce high quality of gold nanorods having reproducible quality and least by-products (spherical or irregular-shaped gold nanoparticles) as evident from the TEM picture.

Figure 10. (**A**) Injection of reagents into Rotating Tube processor (RTP) and Residence Time Unit fitted with an on-line UV monitoring system; (**B**) UV-Vis Spectrum of Gold Nanorods produced over 19 days; (**C**) TEM photographs of the produced GNRs. Adapted from Ref. [53] (with permission from Royal society of Chemistry).

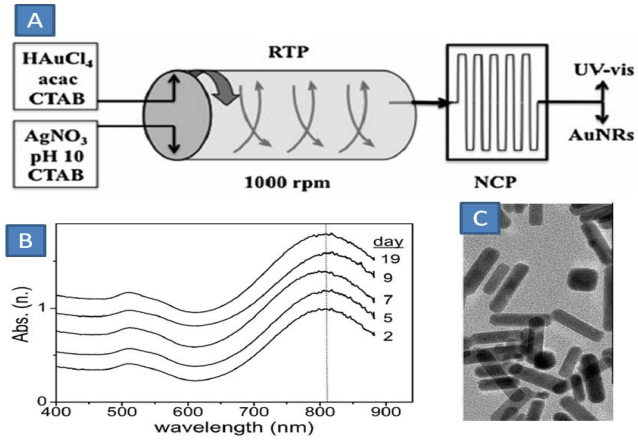

In the "seedless" method, a gold precursor solution ($HAuCl_4$, CTAB, acetylacetone) and a reactant mixture (CTAB, pH 10 carbonate buffer and $AgNO_3$) were fed into the RTP (30 cm × 6 cm, rotating at 1000 rpm). The centrifugal force of the RTP generated a dynamic thin film (300 μm) on the inner wall of the reactor facilitating the Au-seed formation in 30 s. These seeds subsequently grew to nanorods of 24.2 nm × 6.6 nm in the microfluidic chip. Typically, the control of shape and size of anisotropic gold nanoparticles is accomplished by adjusting the concentration of shape modulating agents: silver and CTAB capping agents. By varying the silver concentrations in the second feed, the authors were able

to control the aspect ratio of the produced rods. Although, such capping agents enable synthesis of high quality GNRs, both Ag and CTAB exhibit *in vivo* cytotoxicity, limiting their direct use in biological systems.

In an attempt to create a CTAB and Ag-free variant of anisotropic GNRs synthesis, Sebastian *et al*. presented a Y-mixer connected to a 760 µm i.d.; internal diameter PTFE microreactor for continuous flow synthesis of biocompatible GNRs using amino acid (Lysine) instead of CTAB [54]. The presence of two amino groups in Lysine molecule serves a dual purpose of capping and bridging, which is essential for anisotropic growth of gold particles. A premixed solution of gold salt, potassium carbonate and Lysine was contacted for 10 min with sodium borohydride solution in the microreactor placed in an ultrasonic bath (Figure 11). GNRs are obtained with high monodispersity with microreactor (Figure 11B,C,E) while GNPs with irregular shapes and polydispersity were obtained in benchmark experiments in a batch reactor (Figure 11A,D). Fast mixing between the reactants is attributed to such pronounced difference between conventional and flow reactors. The produced GNRs were biocompatible and exhibited strong absorption in the near-infrared range. These GNRs were successfully used in photothermal optical coherence tomography (OCT) of human breast tissue.

Figure 11. Upper panel: Schematic of Microfluidic setup for CATB and Ag-free Gold Nanorods synthesis. Lower panel: (**A**) Irregular-shaped Gold Nanoparticles from Batch experiments; (**B**) Gold nanorods from microfluidic experiment; (**C**) Absorption spectra of GNP produced in batch and continuous microfluidic device; (**D**) Size distribution of GNPs from batch reactor; (**E**) Size distribution of GNRs from microfluidic device. Adapted from Ref. [54] (with permission from Royal society of Chemistry).

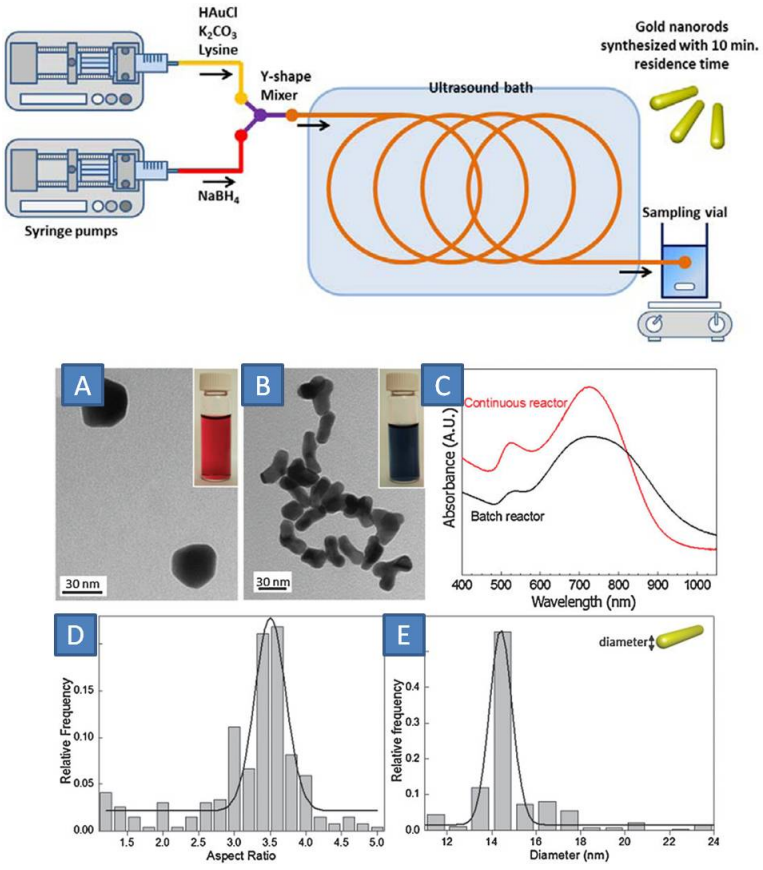

So far, we considered syntheses under single-phase conditions, via controlled mixing and reactions between two or more miscible reagent solutions. This protocol is simple and easily adaptable to different microfluidic set-ups. However, there are several drawbacks associated with single-phase materials synthesis: (1) due to axial diffusion in laminar flow, there exists wide distribution in the residence time (Figure 12A,C), which contributes to polydisperse and intractable mixture of several products and by products [55,56]; (2) mixing occurs solely by diffusion, which requires micromachining of additional structural elements (e.g., pin-fin or split-and-recombine) with lithographic techniques to induce convective flux to assist mixing (Hydrodynamics and reaction studies in a layered herringbone channel [57]; (3) deposition of gold nanoparticles occurs onto the inner reactor walls. The deposit serves as nucleation sites hence depleting feed stock in an unproductive way. The reactor becomes unusable at longer reaction times, which impedes the utility of the reactor for long-term use. Passivation of the channel surface with hydrophobic functional groups was proposed as a possible remedy; however, such methods are not generic for all materials used for microfluidic device fabrication. Specifically, while PDMS is the most widely used materials for microfluidic reactor fabrication, unfortunately PDMS is unsuitable for such chemical passivation.

Figure 12. Cartoons for liquid flow pattern and velocity dispersion in liquid elements for (**A**) one-phase laminar flow, (**B**) water-in-oil droplet flow. Residence time distribution in (**C**) laminar flow and (**D**) droplet flow regimes. Adapted from Ref. [55] (with permission from Wiley-VCH).

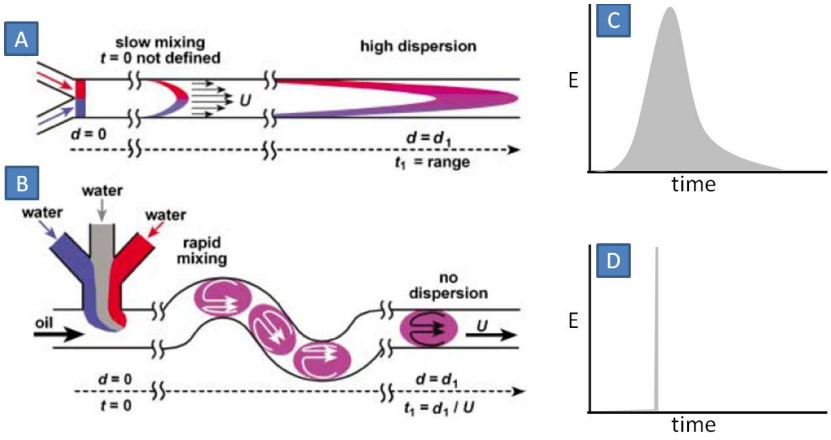

12. Multiphase Flow Operation

Two Phase Segmented Flow

Multiphase flows are created when two of more partially or immiscible fluids are brought in contact. Multiphase flow operation provides several mechanisms for enhancing and extending the performance of single phase microfluidic systems [58,59]. The long diffusion times and dispersion limitations often associated with single-phase flow can be reduced or eliminated by adding a second, immiscible, fluid stream that enhances mixing via transverse convection by inducing a recirculation motion in the liquid. The multiphase flow prevents direct contact between a liquid containing GNPs and the inner microchannel walls and thereby eliminates undesired clogging of channels due to deposition of material on wall surfaces.

In many multiphase operations, reagents containing aqueous streams are pumped inside the microfluidic mixing port/junction and are segmented into small droplets or slugs by introducing an immiscible, non-reacting fluid (gas or oil) [60]. Such droplets/slugs translate through the channel. Due to internal circulation inside these liquid segments, intense inter-phase mixing becomes possible in addition to molecular diffusion. Hence, excellent mixing is accomplished in the segmented flow, which produces a very narrow residence time distribution profile. Moreover, droplets/slugs are produced in high frequency and fidelity in terms of their content concentrations, volume where all droplets act as identical reaction flasks, which are essential to reduce polydispersity and in many cases require minimal/no post-purification operation. All these beneficial attributes of multi-phase microfluidics enabled synthesis of nanoparticles of superior quality and wide chemical-structural diversity [23–25,61]. In the following section, we discuss recent advances in multiphase microfluidics for gold nanoparticles synthesis.

Figure 13. (**1**) Aqueous reagents dispensing in microfluidic channel as water-in-oil droplets; (**2**) Schematic of Microfluidic set-up; (**3**) TEM photographs of produced GNRs of different aspect ratios [decreasing aspect ratios in the order from (**a**) to (**d**)]. Adapted from Ref. [62] (with permission from Wiley-VCH).

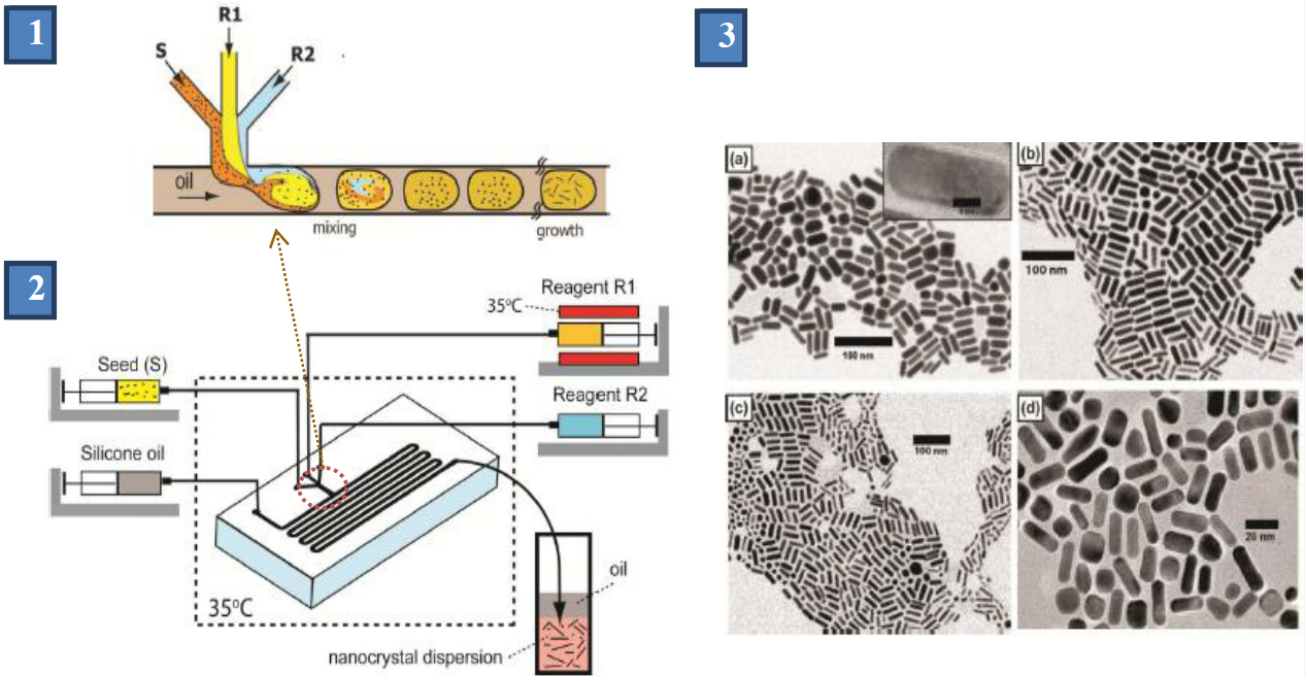

Anisotropic gold nanoparticles, namely gold nanorods, Au-silica core-shell nanomaterials and ultra-small gold nanoparticles were synthesized by Duraiswamy and Khan in segmented flow operation in PDMS-made (Polydimethyloxysiloxane) microchannels [62]. They demonstrated that precise and rapid micromixing within droplets furnished high quality GNRs. Three separate streams containing (1) preformed gold seeds denoted as S (<2 nm); (2) mixture of Au^{3+}, Ag^{+} and CTAB (R1) and (3) ascorbic acid solution (R2) were premixed in a micromixer and then fed into the second micromixer where Taylor flow was created by addition of a silicone oil stream (Figure 13 panel: 1 and 2). Due to intense recirculation inside each droplet, the growth of seeds into rods occurred in a reproducible way, which in turn produced monodisperse GNRs, with insignificant amount of by-products (irregular

colloidal gold). By manipulating silver content in the droplets, GNRs of different aspect ratios were produced (Figure 13; panel 3). The reactor was used for 12 h without any channel fouling.

In GNRs synthesis, reliable and continuous supply of stabilized ultra-small gold nanoparticles (or seeds) is of importance to realize a reliable production facility. As discussed in the first part of this review, several authors attempted microfluidic synthesis of ultra-small GNPs using a strong reducing agent, sodium borohydride. However, sodium borohydride is known to decompose in water and produce hydrogen gas bubbles. Generation of additional gas phase in single phase operation may enhance convective mixing between liquid elements, however in a rather irregular manner [32]. Such unpredictable and irregular mixing between liquid reactants would make the process unreliable for sustained and reproducible synthesis. Saif *et al*. suggested to use gas-liquid flow in which nitrogen bubbles were introduced to absorb hydrogen released from the sodium borohydride solution (Figure 14A,B) [63]. In this system, hydrogen gas forming in the aqueous phase rapidly diffuse into the intervening nitrogen bubbles due to large concentration gradient and intense vortex in the liquid slugs. Thereby, hydrogen concentration in the aqueous phase was kept well below the saturation point to suppress nucleation and micro bubbles formation inside the aqueous slugs. A diffusion model was developed which showed that the hydrogen concentration in liquid remained below the solubility threshold of 0.9 mM. In that way, the process was run for 8 h. Spherical gold nanocrystals of below 5 nm in size were produced (Figure 14C). These seeds were successfully used to produce high quality GNRs in batch synthesis. This work envisages that a full continuous process of seed formation and subsequent use in GNRs synthesis would be possible without any flow mal-distribution by $NaBH_4$ decomposition.

Figure 14. (**A**) Schematic of gas-liquid segmented flow generation and hydrogen gas dissolution from aqueous slugs into gas bubbles; (**B**) Microscopic photograph of gas-liquid segmented flow; (**C**) Microfluidic set-up for <5 nm gold seed formation by gas-liquid segmentation and hydrogen-gas trapping. Adapted from Ref. [63] (with permission from Royal Society of Chemistry).

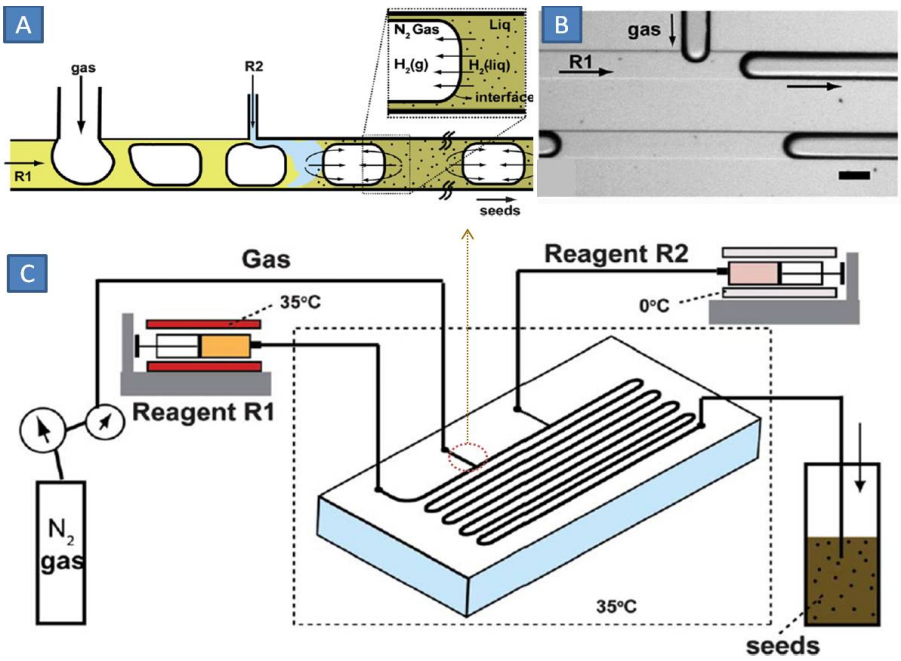

In a similar way, Jensen *et al*. created slugs of aqueous phase containing gold precursor and sodium borohydride solution inside a silicone-pyrex chip by adding either silicone oil, toluene or air as immiscible fluid (Figure 15) [64]. The mixing zone was kept at room temperature while the reaction zone (100 μL volume, either hydrophilic or hydrophobic walls) was kept at 100 °C. In the hydrophilic channel network, continuous aqueous slugs were created inside the channel by introducing the immiscible fluid. In this case, all aqueous slugs were connected to each other by a thin film. The length of the aqueous slugs had pronounced effect on the product size and polydispersity. Short slugs in toluene produced smaller particles of 3.8 ± 0.3 nm at a residence time of 10 s while longer slugs gave larger particles of 4.9 ± 3.0 nm with significant polydispersity at a residence time of 40 s. The relative slip velocity between continuous phase and aqueous slugs determined the internal mixing within the slugs and polydispersity. They observed that higher slip velocity produced narrow particle size distribution, while lower slip velocity lead to poor mixing and wide particle size distribution. The authors derived a relationship between the slug length and the particle size (and polydispersity) in terms of inter-slug mass transfer, which is a function of the slug length.

In the hydrophobic channel network, the droplets of aqueous phase were separated from each other by the continuous organic (or air) phase. They showed that axial dispersion was drastically reduced.

Figure 15. (**a**) Schematic of segmented flow generation in a hydrophilic channel; (**b**) photograph of aqueous slugs in toluene (aqueous slugs are dyed with fluorescein for better visualization); (**c**) microchip with cold (for mixing) and hot zones (for reaction). Adapted from Ref. [64] (with permission from American Chemical Society).

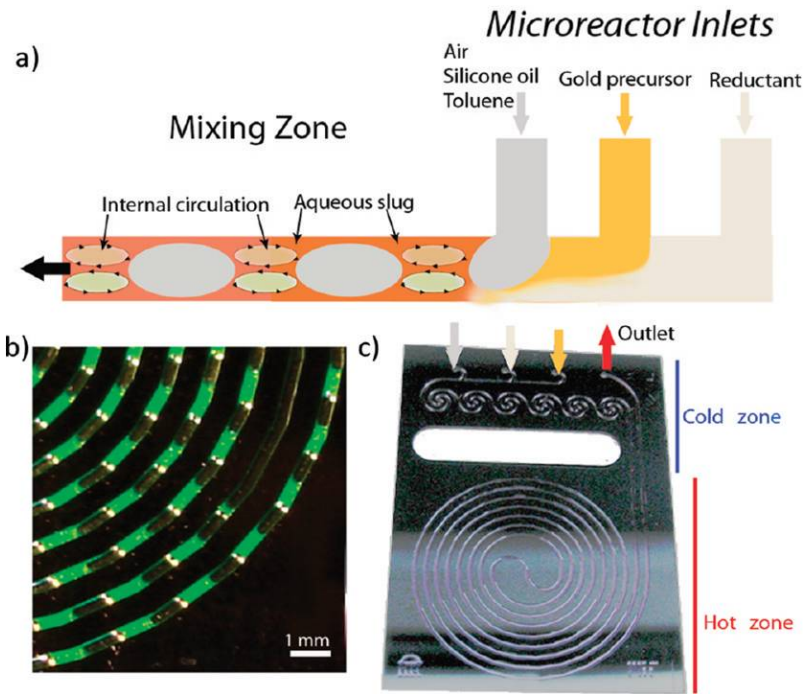

13. Three Phase Segmented Flow

Three phase segmented flow of inert gas, reactant containing aqueous droplets dispersed in a continuous oil phase was employed inside a microchannel by Duraiswamy *et al*. to produce SiO_2@Au core-shell materials with variable plasmonic behavior (600–900 nm in absorption spectrum) [65]

(Figure 16). In this approach, inlet clogging due to particle deposition was avoided and droplet coalescence was considerably reduced. The gold coverage onto the silica particles was controlled by the inlet flow rates. Moreover, uncontrolled formation of free gold outside the surface of seeded-silica particles was largely avoided, which enabled pure batches of core-shell materials of varying plasmonic signatures.

Figure 16. (**1**) Microfluidic formation of gas-aqueous foam in continuous oil; (**2**) Panel showing TEM photographs of (**a**) gold-seeded silica particles, (**b**) small gold island on silica, (**c**) dense gold islands on silica, (**d**) fully developed gold shell on silica spheres, (**e**) inset showing UV-Vis absorption of the particles (**a**)–(**d**). Adapted from Ref. [65] (with permission from American Chemical Society).

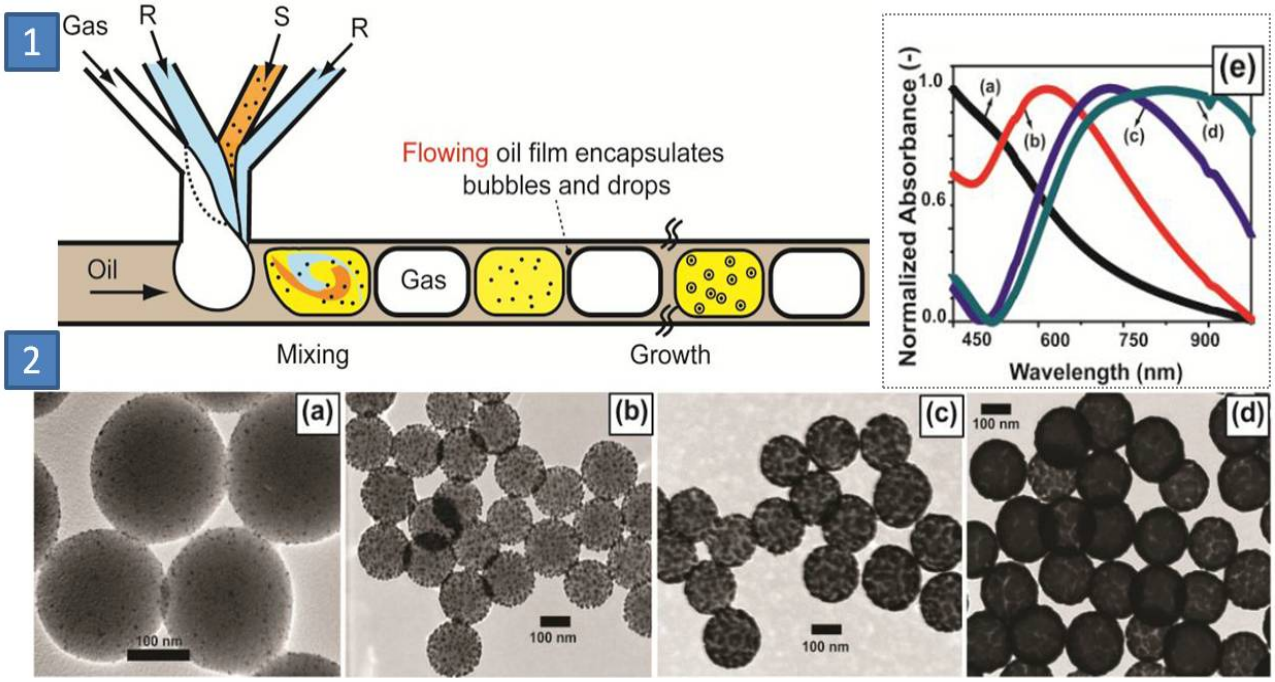

In majority of work, liquid-based *i.e.*, aqueous solutions of reducing agents such as ascorbic acid, trisodium citrate, sodium borohydride *etc*. are used in redox-based nanomaterials syntheses. Carbon monoxide or hydrogen are cleaner variants of the reducing agents and can be separated from the reaction mixture by mere exposing to ambient atmosphere. Several groups utilized gaseous reactants in nanomaterials synthesis [66–68], including gold nanoshell synthesis [69]. As the size of GNPs depends on kinetics on nucleation and growth, any inhomogeneity during gas-liquid mass-transport would render the synthesis unreliable and irreproducible. Multiphase microchemical systems take advantage of the large interfacial areas. Carbon monoxide was used as reducing agent to produce SiO_2@Au nanomaterials in a PDMS-membrane microreactor by Rahman *et al*. (Figure 17A) [70]. In this way, CO was dissolved inside the aqueous droplets without forming any gas bubbles. (Figure 17B,C). Depending on the residence time of aqueous droplets (1–70 s), the flow rate of CO across the membrane was adjusted to control the rate of gold deposition onto the silica core. In this way, SiO_2@Au nanomaterials with variable gold coverage and impressively high purity (free from colloidal gold) were produced (Figure 17D). Rapid quenching of the gold deposition was possible by eliminating gas/liquid contact in the downstream section.

Figure 17. (**A**) Microfluidic set-up for water-oil droplet formation; Schematic (**B**) and microscopic photograph (**C**) of gas-liquid contacting across the membrane; (**D**) Core-shell formation with variable gold coverage (**a**–**d**). Adapted from Ref. [70] (with permission from Royal Society of Chemistry).

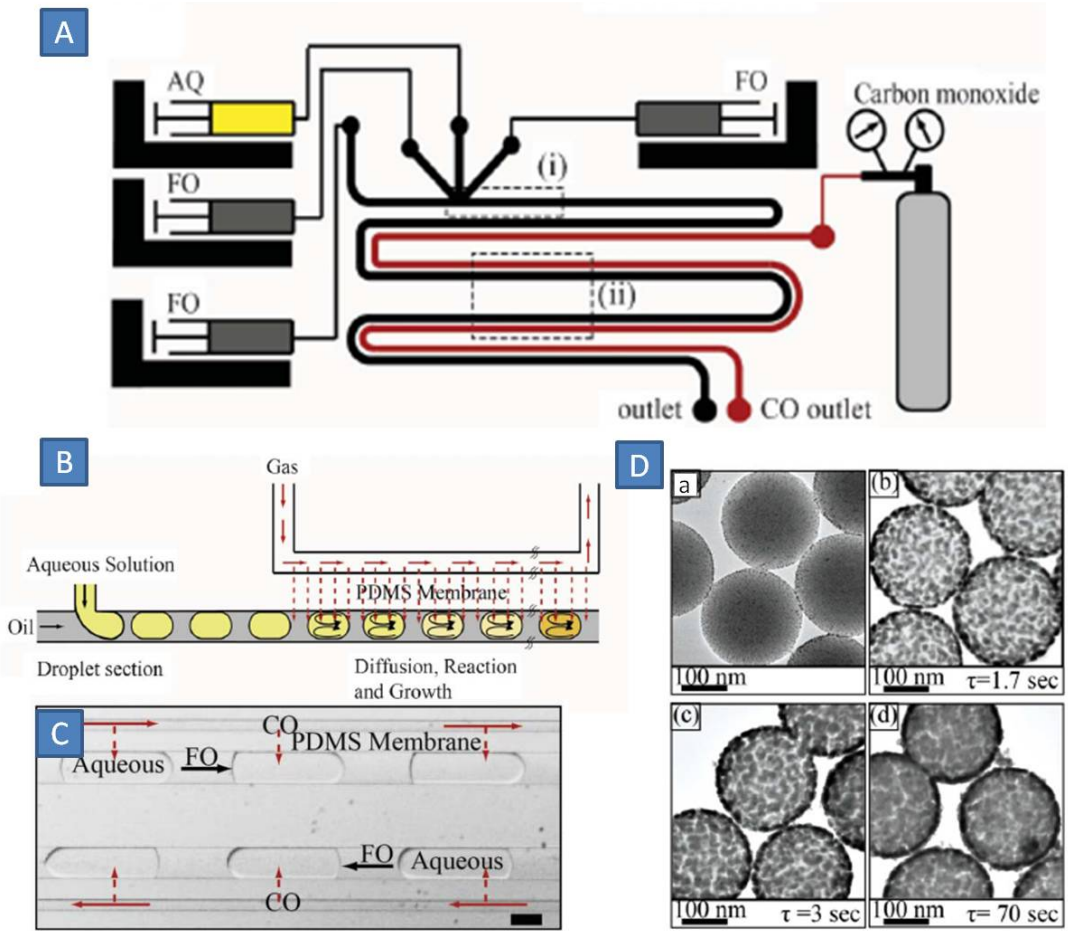

14. Application of Ionic Liquids

Recently, ionic liquids (IL) are considered as an alternative reaction medium for nanoparticles synthesis, given their unique molecular nature, polarity and ability to stabilize nanoparticles via numerous modes of interactions [71–73]. Ionic liquids may serve a dual purpose as a solvent and molecular/colloidal stabilizer, however GNPs synthesis in IL is challenging in terms of size distribution, presumably due to poor mass transport in viscous ionic liquids.

Lazarus *et al*. leveraged the beneficial attributes of both ionic liquids and microreactors for the synthesis of GNPs [74]. The authors used a flow-focusing microfluidic protocol where in the mixing zone a stream of butyl methylimidazolium tetrafluoroborate (BMIM-BF_4) was injected between the two reactant streams ($HAuCl_4$/1-methylimidazole and $NaBH_4$ in BMIM-BF_4) to allow fast mixing (Figure 18A). As this stream arrived at a flow-focusing cross-junction, two oil streams were fed orthogonal to the IL streams. At oil flow rates below 3000 μL h^{-1}, the middle IL stream maintained co-parallel flow with the flanking oil streams (inset A in Figure 18), while above this threshold value, droplets of IL were formed (Inset B in Figure 18). Fast and homogeneous mixing enable rapid nucleation burst, and ensure monodispersity in the final fully grown GNPs. The liquid mixture was

quenched at the outlet with ethanol to separate the produced GNPs and analyzed by spectroscopic and microscopic methods. The best quality GNPs in terms of polydispersity (12%), size and roundedness of the GNPs was achieved from the droplet protocol. The mean particle diameter was 4.38 ± 0.53 nm having spherical features. The roundness, defined as (4 × particle area)/(π × (major axis length)^2), below 0.85 was observed only in 15% particles. UV-vis spectra of suspensions exhibited narrow surface plasmon bands cantered at 518.5 nm, typical of non-agglomerated GNPs. With the parallel flow protocol, the GNPs were of inferior structural features compared to droplet protocol. The mean diameter was 5.65 ± 1.03 nm with a polydispersity index of 18.2%. The roundness below 0.85 was observed in 23% particles. Intriguingly, thinning of the innermost lamella (IL liquid) by increasing the oil flow rate showed tendency of the GNPs to become more monodispersed compared to the case when the inert oil phase was completely excluded. Understandably, mixing within droplets is most efficient due to intense vortex generation, while interdiffusion between liquid streams become progressively limited as the characteristic dimension of the lamella becomes larger. In all cases, the synthesis was completed in 19 s. A benchmarking experiment in the batch requires at least 1 min. The obtained nanoparticles were significantly spheroidal with 28% having a roundness less than 0.85. The mean diameter was larger than that in the flow synthesis (6.25 ± 1.29 nm; polydispersity: 20.6%).

Figure 18. Schematic of the PDMS device (3 × 5 cm) with flow focusing geometry. channel widths and depths are 600 μm and 95 μm (flow-focusing region width: 400 μm), respectively, with a total channel volume of 7.6 μm. Inset **A**: parallel flow of IL and inert Oil at Oil flow rates below 3000 μL h^{-1}, inset **B**: IL droplet formation at Oil flow rates beyond 3000 μL h^{-1}. Adapted from Ref. [74] (with permission from Royal Society of Chemistry).

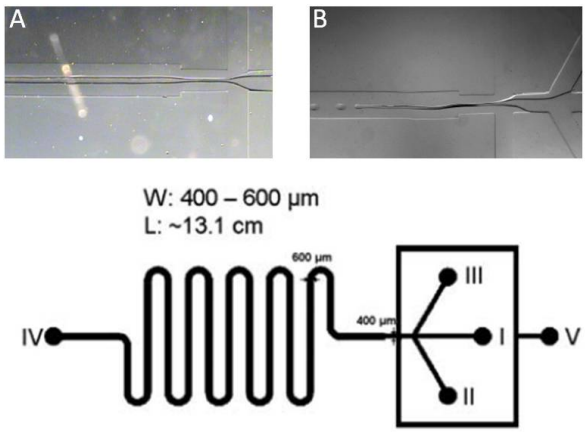

Larazus *et al*. later reported the use of ionic liquid variant of sodium borohydride, namely, 1-butyl-1-methylimidazolium borohydride (BMIM BH_4), to increase the solubility of reducing agent in butyl methylimidazolium bis-triflamide ionic liquid (BMIM NTf_2) in the synthesis of GNPs in a fluorinated PDMS channel [75]. The dispersed phase contained the IL reducing agent and gold ions while a fluorocarbon oil was continuous phase. At low ionic liquid/oil flow ratios of 0.05–0.25, droplets were formed immediately at the junction location. In comparison to batch conditions their microfluidic method produced GNPs of smaller size and higher monodispersity.

15. Scale-Up of GNP Synthesis Using Flow-Chemistry

Only few reports emerged that tackles the scale-up issue associated with complex gold nanoparticles production. Gomez *et al*. presented the first example of continuous synthesis of hollow GNPs in a flow reactor composed of T-pieces for mixing and a 1.6 mm diameter PTFE tube as residence time unit at two different scales corresponding to production rates of 0.2 and 2.0 mmol Au/min [76]. Hollow GNPs exhibit plasmonic behavior, where the ratio of particle diameter to the thickness of the shell determines the surface plasmon resonance (SPR) peak position and their uniformity determines the SPR bandwidth. At first, a cobalt solution was mixed with sodium borohydride in the first T-junction which produced cobalt nanospheres within 180 s of reaction time (Figure 19). This step was diffusion limited, and the reaction time was set slightly higher than the diffusive mixing time of 160 s. In the second mixer, a gold precursor was introduced which was reduced at the surface of cobalt particles which in turn was dissolved out after being oxidized. In the scale-up process, a stream of oxygen was introduced in the 3rd mixing port to facilitate this galvanic dissolution process to form completely Co free hollow GNPs. *In-situ* functionalization of hollow GNPs with thiolated polyethylene glycols was demonstrated to enhance the biocompatibility. An integrated continuous UV sterilization step facilitated the on-site *in vivo* use of the as-synthesized materials. Such integration of continuous production and downstream processing in a millireactor holds promises for scaling up of "ready-to-use" nanoparticles production.

Figure 19. Microfluidic schematic of hollow gold nanoparticles in a multi-step approach with average reaction time for each step. Insets are TEM photographs of the corresponding nanoparticles formed throughout the process at different stages. Adapted from Ref. [76] (with permission from Royal Society of Chemistry).

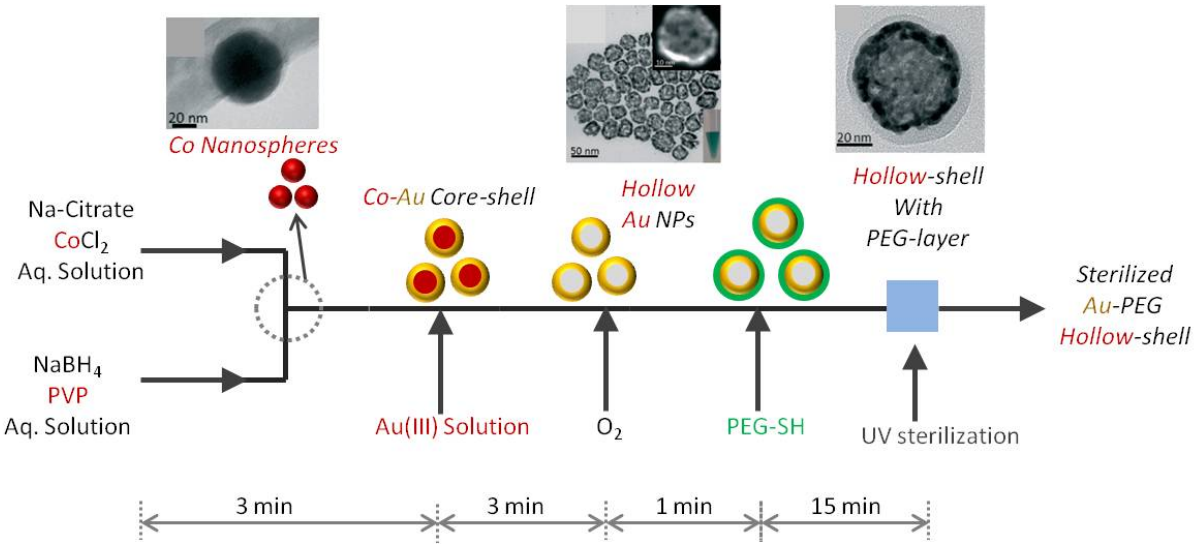

Lohse *et al*. scaled up the microfluidic synthesis to produce 10 L of suspension of GNRs with aspect ratio 2 in three consecutive runs amounting to a total of 1.0 g of product [77]. The product yield and quality showed improvement in regards to monodispersity when compared to the synthesis in a batch system. This clearly shows superiority of microfluidic synthesis over conventional bath synthesis that typically produces 50 mg of GNPs. This was possible using 5–10 fold higher concentrations of

reactants in the flow system. Off-the shelf materials were used to construct the fluidic reactor, namely from TYGON polyvinyl tubing as the reactor and polyethylene connectors as mixing ports. In the first step, CTAB-stabilized spherical GNPs were sued via rapid reduction of gold with $NaBH_4$ was conducted in the flow reactor that produces GNPs that would be used as seed elements in the GNRs synthesis. In the second stage, these seeds were mixed with a growth solution containing (gold salt, CTAB, silver nitrate and ascorbic acid) to generate the rods of tight batch-quality (in terms of desired shape-size and avoidance of undesired by-products). By changing concentrations GNRs with different length (and aspect ratios were obtained. They produce a wide range of plasmonic bands up to near infrared region (Figure 20).

Figure 20. (**A**) UV-Vis spectrum of GNRs of various aspect ratios; (**B**) TEM Photographs of GNRs, inset showing the simple T-junction used as micromixer in this work [variable aspect ratios of the produces gold nanorods are shown in (i)-(v)]. Adapted from Ref. [77] (with permission from American Chemical Society).

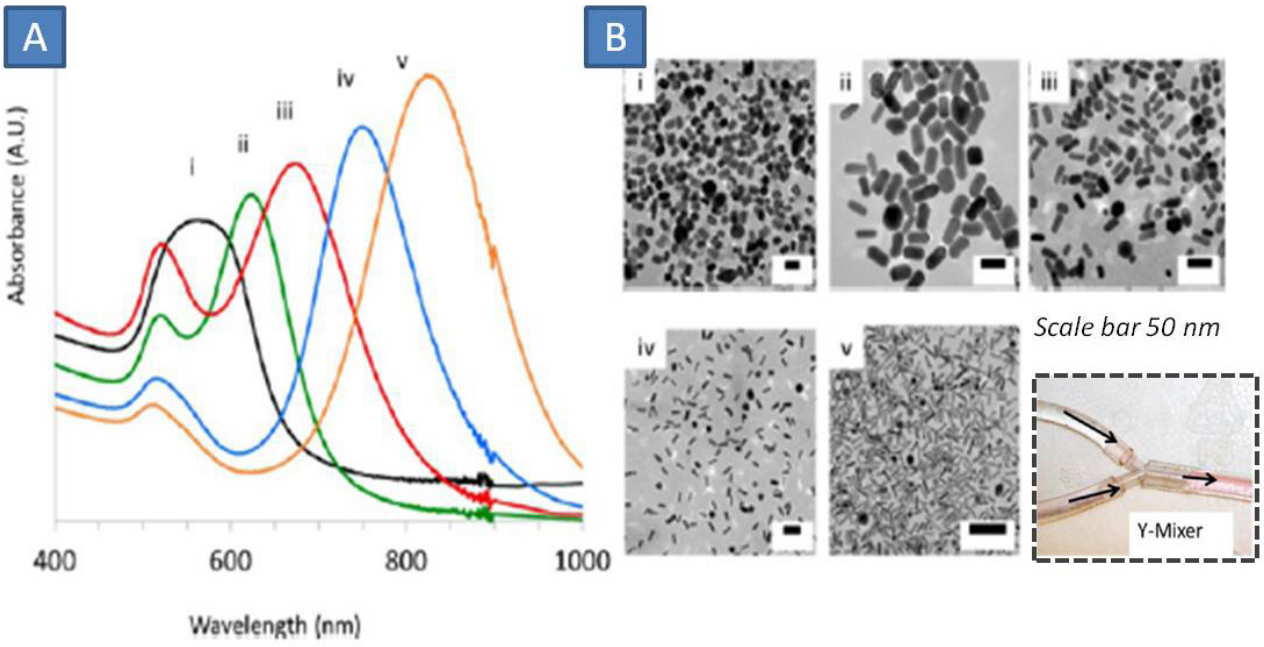

16. Concluding Remarks

Multiphase microreactors have proven particularly promising in the synthesis of complex Au nanoparticles with high monodispersity within short timescales. The precise manipulation of bubbles, droplets or immiscible fluid streams in microfluidic chips is usually achieved by elaborate chip designs that address fluid-fluid hydrodynamics under laminar flow conditions and fluid-solid interactions in microchannels. Such conditions enable fast heating and quenching of reaction mixture under well-defined hydrodynamic conditions. Scale-up is a necessary step when going from mg/day to g/day production rate. The scale-up of multiphase flow remains a major challenge in current microfluidic applications. It often requires application of on-line measurement techniques to monitor the slug lengths, and other dynamic parameters such as flow reversals in order to provide fast feedback to a process control system.

Gas-liquid-liquid three-phase flow in microfluidic systems still remains as a less explored area and has received growing interests in recent years due to its important implications for the synthesis of gold nanoparticles. The use of an inert gas to break up an otherwise liquid-liquid segmented or parallel flow in microchannels yields a better quality of obtained nanomaterials. Hydrodynamics of three phase (gas-liquid-liquid) flow is not yet fully understood. There exist a rather limited number of publications dealing with the design and operation of three-phase flow in microchannels, however the microfluidic systems being far from fully optimized. This is largely due to the current inadequate understanding on the underlying hydrodynamics. The fundamental laws governing the three-phase generation and flow in microchannels are not yet understood due to their complex nature. The influence of flow rate on the size of bubbles or droplets produced under a three-phase flow has been revealed with some empirical correlations. However, the influence of other parameters, such as fluid properties and the geometry of inlet mixer, were rarely taken into account.

The large interfacial areas associated with multiphase microflows provide efficient mass transfer between immiscible fluids. This opens up new perspective to replace aggressive reducing agent with reactive gases, which would allow making a step forward towards green process engineering.

Acknowledgments

The financial support provided by the European Research Council (ERC) project 279867, is gratefully acknowledged. We thank Yanging Jing for help in the literature survey.

Conflicts of Interest

The authors declare no conflict of interest.

References

1. Huaizhi, Z.; Yuantao, N. China's Ancient Gold Drugs. *Gold Bull.* **2001**, *34*, 24–29.
2. Brown, C.L.; Whitehouse, M.W.; Agarwal, D.S.; Tupe, S.G.; Paknikar, K.M.; Teiknik, E.R.T. Nanogoldpharmaceutics. *Gold Bull.* **2007**, *40*, 245–250.
3. Daniel, M.-C.; Astruc, D. Gold Nanoparticles: Assembly, Supramolecular Chemistry, Quantum-Size-Related Properties, and Applications Toward Biology, Catalysis, and Nanotechnology. *Chem. Rev.* **2004**, *104*, 293–346.
4. Faraday, M. The Bakerian Lecture: Experimental Relations of Gold (and Other Metals) to Light. *Philos. Trans. R. Soc. Lond.* **1857**, *147*, 145–181.
5. Turkevich, J.; Hillier, J. Electron Microscopy of Colloidal Systems. *Anal. Chem.* **1949**, *21*, 475–485.
6. Turkevich, J.; Stevenson, P.C.; Hillier, J. A study of Nucleation and Growth Processes in the Synthesis of Colloidal Gold. *Discuss. Faraday Soc.* **1951**, *11*, 55–75.
7. Boisselier, E.; Astruc, D. Gold Nanoparticles in Nanomedicine: Preparations, Imaging, Diagnostics, Therapies and Toxicity. *Chem. Soc. Rev.* **2009**, *38*, 1759–1782.
8. Chen, H.; Shao, L.; Li, Q.; Wang, J. Gold Nanorods and Their Plasmonic Properties. *Chem. Soc. Rev.* **2013**, *42*, 2679–2724.

9. Cobley, C.M.; Chen, J.; Cho, E.C.; Wang, L.V.; Xia, Y. Gold Nanostructures: A Class of Multifunctional Materials for Biomedical Applications. *Chem. Soc. Rev.* **2011**, *40*, 44–56.
10. Corma, A.; Garcia, H. Supported Gold Nanoparticles as Catalysts for Organic Reactions. *Chem. Soc. Rev.* **2008**, *37*, 2096–2126.
11. Doane, T.L.; Burda, C. The Unique Role of Nanoparticles in Nanomedicine: Imaging, Drug Delivery and Therapy. *Chem. Soc. Rev.* **2012**, *41*, 2885–2911.
12. Dreaden, E.C.; Alkilany, A.M.; Huang, X.; Murphy, C.J.; El-Sayed, M.A. The Golden Age: Gold Nanoparticles for Biomedicine. *Chem. Soc. Rev.* **2012**, *41*, 2740–2779.
13. Eustis, S.; El-Sayed, M.A. Why Gold Nanoparticles Are More Precious Than Pretty Gold: Noble Metal Surface Plasmon Resonance and Its Enhancement of the Radiative and Nonradiative Properties of Nanocrystals of Different Shapes. *Chem. Soc. Rev.* **2006**, *35*, 209–217.
14. Hutchings, G.J.; Brust, M.; Schmidbaur, H. Gold—An Introductory Perspective. *Chem. Soc. Rev.* **2008**, *37*, 1759–1765.
15. Lee, D.-E.; Koo, H.; Sun, I.-C.; Ryu, J.H.; Kim, K.; Kwon, I.C. Multifunctional Nanoparticles for Multimodal Imaging and Theragnosis. *Chem. Soc. Rev.* **2012**, *41*, 2656–2672.
16. Li, G.; Jin, R. Atomically Precise Gold Nanoclusters as New Model Catalysts. *Acc. Chem. Res.* **2013**, *46*, 1749–1758.
17. Llevot, A.; Astruc, D. Applications of Vectorized Gold Nanoparticles to the Diagnosis and Therapy of Cancer. *Chem. Soc. Rev.* **2012**, *41*, 242–257.
18. La Mer V.K.; Dinegar, H. Theory, Production and Mechanism of Formation of Monodisperse Hydrosols. *J. Am. Chem. Soc.* **1950**, *72*, 4847–4854.
19. Polte, J.; Tuaev, X.; Wuithschick, M.; Fischer, A.; Thuenemann, A.F.; Rademann, K.; Kraehnert, R.; Emmerling, F. Formation Mechanism of Colloidal Silver Nanoparticles: Analogies and Differences to the Growth of Gold Nanoparticles. *ACS Nano* **2012**, *6*, 5791–5802.
20. Hessel, V.; Hardt, S.; Löwe, H. *Chemical Micro-Process Engineering*; Wiley-VCH: Weinhein, Germany, 2004.
21. Reschetilowski, W. *Microreactors in Preparative Chemistry*; Wiley-VCH: Weinhein, Germany, 2013.
22. Wirth, T. *Microreactors in Organic Chemistry and Catalysis*; Wiley-VCH: Weinhein, Germany, 2013.
23. Abou-Hassan, A.; Sandre, O.; Cabuil, V. Microfluidics in Inorganic Chemistry. *Angew. Chem. Int. Ed. Engl.* **2010**, *49*, 6268–6286.
24. Marre, S.; Jensen, K.F. Synthesis of Micro and Nanostructures in Microfluidic Systems. *Chem. Soc. Rev.* **2010**, *39*, 1183–1202.
25. Song, Y.; Hormes, J.; Kumar, C.S.S.R. Microfluidic Synthesis of Nanomaterials. *Small* **2008**, *4*, 698–711.
26. Navin, C.V.; Krishna, K.S.; Theegala, C.S.; Kumar, C.S.S.R. Lab-on-a-Chip Devices for Gold Nanoparticle Synthesis and Their Role as a Catalyst Support for Continuous Flow Catalysis. *Nanotechnol. Rev.* **2013**, doi:10.1515/ntrev-2013-0028.
27. Wagner, J.; Kirner, T.; Mayer, G.; Albert, J.; Köhler, J. Generation of Metal Nanoparticles in a Microchannel Reactor. *Chem. Eng. J.* **2004**, *101*, 251–260.

28. Wagner, J.; Köhler, J.M. Continuous Synthesis of Gold Nanoparticles in a Microreactor. *Nano Lett.* **2005**, *5*, 685–691.
29. Köhler, J.M.; Wagner, J.; Albert, J. Formation of Isolated and Clustered Au Nanoparticles in the Presence of Polyelectrolyte Molecules Using a Flow-through Si-Chip Reactor. *J. Mater. Chem.* **2005**, *15*, 1924–1930.
30. Wagner, J.; Tshikhudo, T.; Kohler, J. Microfluidic Generation of Metal Nanoparticles by Borohydride Reduction. *Chem. Eng. J.* **2008**, *135*, S104–S109.
31. Haruta, M.; Yamada, N.; Kobayashi, T.; Iijima, S. Gold Catalysts Prepared by Co-Precipitation for Low-Temperature Oxidation of Hydrogen and of Carbon Monoxide, *J. Catal*. **1989**, *115*, 301–309.
32. Tsunoyama, H.; Ichikuni, N.; Tsukuda, T. Microfluidic Synthesis and Catalytic Application of PVP-Stabilized, Approximately 1 nm Gold Clusters. *Langmuir* **2008**, *24*, 11327–11330.
33. Luty-Błocho, M.; Fitzner, K.; Hessel, V.; Löb, P.; Maskos, M.; Metzke, D.; Pacławski, K.; Wojnicki, M. Synthesis of Gold Nanoparticles in an Interdigital Micromixer Using Ascorbic Acid and Sodium Borohydride as Reducers. *Chem. Eng. J.* **2011**, *171*, 279–290.
34. Ishizaka, T.; Ishigaki, A.; Kawanami, H.; Suzuki, A.; Suzuki, T.M. Dynamic Control of Gold Nanoparticle Morphology in a Microchannel Flow Reactor by Glucose Reduction in Aqueous Sodium Hydroxide Solution. *J. Colloid Interface Sci.* **2012**, *367*, 135–138.
35. Jun, H.; Fabienne, T.; Florent, M.; Coulon, P.; Nicolas, M.; Olivier, S. Understanding of the Size Control of Biocompatible Gold Nanoparticles in Millifluidic Channels. *Langmuir* **2012**, *28*, 15966–15974.
36. Gómez-de Pedro, S.; Puyol, M.; Alonso-Chamarro, J. Continuous Flow Synthesis of Nanoparticles Using Ceramic Microfluidic Devices. *Nanotechnology* **2010**, *21*, 415603.
37. Ftouni, J.; Penhoat, M.; Addad, A.; Payen, E.; Rolando, C.; Girardon, J.-S. Highly Controlled Synthesis of Nanometric Gold Particles by Citrate Reduction using the Short Mixing, Heating and Quenching Times Achievable in a Microfluidic Device. *Nanoscale* **2012**, *4*, 4450–4454.
38. Sugie, A.; Song, H.; Horie, T.; Ohmura, N.; Kanie, K.; Muramatsu, A.; Mori, A. Synthesis of Thiol-Capped Gold Nanoparticle with a Flow System Using Organosilane as a Reducing Agent. *Tetrahedron Lett.* **2012**, *53*, 4457–4459.
39. Krishna, K.S.; Navin, C.V.; Biswas, S.; Singh, V.; Ham, K.; Bovenkamp, G.L.; Theegala, C.S.; Miller, T.; Spivey, J.J.; Kumar, C.S.S.R. Millifluidics for Time-Resolved Mapping of the Growth of Gold Nanostructures. *J. Am. Chem. Soc.* **2013**, *135*, 5450–5456.
40. Cortie, M.B.; McDonagh, A.M. Synthesis and Optical Properties of Hybrid and Alloy Plasmonic Nanoparticles. *Chem. Rev.* **2011**, *111*, 3713–3735.
41. Ghosh Chaudhuri, R.; Paria, S. Core/shell Nanoparticles: Classes, Properties, Synthesis Mechanisms, Characterization, and Applications. *Chem. Rev.* **2012**, *112*, 2373–2433.
42. Grzelczak, M.; Pérez-Juste, J.; Mulvaney, P.; Liz-Marzán, L.M. Shape Control in Gold Nanoparticle Synthesis. *Chem. Soc. Rev.* **2008**, *37*, 1783–1791.
43. Halas, N.J.; Lal, S.; Link, S.; Chang, W.-S.; Natelson, D.; Hafner, J.H.; Nordlander, P. A Plethora of Plasmonics from the Laboratory for Nanophotonics at Rice University. *Adv. Mater.* **2012**, *24*, 4842–4877.

44. Hu, M.; Chen, J.; Li, Z.-Y.; Au, L.; Hartland, G.V.; Li, X.; Marquez, M.; Xia, Y. Gold Nanostructures: Engineering Their Plasmonic Properties for Biomedical Applications. *Chem. Soc. Rev.* **2006**, *35*, 1084–1094.
45. Schärtl, W. Current Directions in Core-Shell Nanoparticle Design. *Nanoscale* **2010**, *2*, 829–843.
46. Vigderman, L.; Khanal, B.P.; Zubarev, E.R. Functional Gold Nanorods: Synthesis, Self-Assembly, and Sensing Applications. *Adv. Mater.* **2012**, *24*, 4811–4841.
47. Huang, X.; Neretina, S.; El-Sayed, M. Gold Nanorods: From Synthesis and Properties to Biological and Biomedical Applications. *Adv. Mater.* **2009**, *21*, 4880–4910.
48. Köhler, J.M.; Held, M.; Hübner, U.; Wagner, J. Formation of Au/Ag Nanoparticles in a Two Step Micro Flow-Through Process. *Chem. Eng. Technol.* **2007**, *30*, 347–354.
49. Sun, L.; Luan, W.; Shan, Y.; Tu, S. One-Step Synthesis of Monodisperse Au–Ag Alloy Nanoparticles in a Microreaction System. *Chem. Eng. J.* **2012**, *189–190*, 451–455.
50. Stöber, W.; Fink, A.; Bohn, E. Controlled Growth of Monodisperse Silica Spheres in the Micron Size Range. *J. Colloid Interface Sci*. **1968**, *26*, 62–69.
51. Gomez, L.; Arruebo, M.; Sebastian, V.; Gutierrez, L.; Santamaria, J. Facile Synthesis of SiO_2–Au Nanoshells in a Three-Stage Microfluidic System. *J. Mater. Chem.* **2012**, *22*, 21420.
52. Boleininger, J.; Kurz, A.; Reuss, V.; Sönnichsen, C. Microfluidic Continuous Flow Synthesis of Rod-Shaped Gold and Silver Nanocrystals. *Phys. Chem. Chem. Phys.* **2006**, *8*, 3824.
53. Bullen, C.; Latter, M.J.; D'Alonzo, N.J.; Willis, G.J.; Raston, C.L. A Seedless Approach to Continuous Flow Synthesis of Gold Nanorods. *Chem. Commun. (Camb).* **2011**, *47*, 4123–4125.
54. Sebastián, V.; Lee, S.-K.; Zhou, C.; Kraus, M.F.; Fujimoto, J.G.; Jensen, K.F. One-Step Continuous Synthesis of Biocompatible Gold Nanorods for Optical Coherence Tomography. *Chem. Commun. (Camb).* **2012**, *48*, 6654–6656.
55. Song, H.; Tice, J.D.; Ismagilov, R.F. A Microfluidic System for Controlling Reaction Networks in Time. *Angew. Chem. Int. Ed*. **2003**, *42*, 767–772.
56. Yen, B.K.H.; Günther, A.; Schmidt, M.A.; Jensen, K.F.; Bawendi, M.G. A Microfabricated Gas-Liquid Segmented Flow Reactor for High-Temperature Synthesis: The Case of CdSe Quantum Dots. *Angew. Chem. Int. Ed. Engl.* **2005**, *44*, 5447–5451.
57. Cantu-Perez, A.; Barrass, S.; Gavriilidis, A. Hydrodynamics and reaction studies in a layered herringbone channel. *Chem. Eng. J.* **2011**, *167*, 657–665.
58. Theberge, A.B.; Courtois, F.; Schaerli, Y.; Fischlechner, M.; Abell, C.; Hollfelder, F.; Huck, W.T.S. Microdroplets in Microfluidics: An Evolving Platform for Discoveries in Chemistry and Biology. *Angew. Chem. Int. Ed.* **2010**, *49*, 5846–5868.
59. Teh, S.-Y.; Lin, R.; Hung, L.-H.; Lee, A.P. Droplet Microfluidics. *Lab Chip* **2008**, *8*, 198–220.
60. Baroud, C.N.; Gallaire, F.; Dangla, R. Dynamics of Microfluidic Droplets. *Lab Chip* **2010**, *10*, 2032–2045.
61. Krishna, K.S.; Li, Y.; Li, S.; Kumar, C.S.S.R. Lab-on-a-Chip Synthesis of Inorganic Nanomaterials and Quantum Dots for Biomedical Applications. *Adv. Drug Deliv. Rev.* **2013**, *65*, 1470–1495.
62. Duraiswamy, S.; Khan, S.A. Droplet-Based Microfluidic Synthesis of Anisotropic Metal Nanocrystals. *Small* **2009**, *5*, 2828–2834.

63. Khan, S.A.; Duraiswamy, S. Controlling Bubbles Using Bubbles—Microfluidic Synthesis of Ultra-Small Gold Nanocrystals with Gas-Evolving Reducing Agents. *Lab Chip* **2012**, *12*, 1807–1812.
64. Cabeza, V.S.; Kuhn, S.; Kulkarni, A.A.; Jensen, K.F. Size-Controlled Flow Synthesis of Gold Nanoparticles Using a Segmented Flow Micro Fluidic Platform. *Langmuir* **2012**, *28*, 7007–7013.
65. Duraiswamy, S.; Khan, S.A. Plasmonic Nanoshell Synthesis in Microfluidic Composite Foams. *Nano Lett.* **2010**, *10*, 3757–3763.
66. Huang, X.; Tang, S.; Mu, X.; Dai, Y.; Chen, G.; Zhou, Z.; Ruan, F.; Yang, Z.; Zheng, N. Freestanding Palladium Nanosheets with Plasmonic and Catalytic Properties. *Nat. Nanotechnol.* **2011**, *6*, 28–32.
67. Kang, Y.; Ye, X.; Murray, C.B. Size- and Shape-Selective Synthesis of Metal Nanocrystals and Nanowires Using CO as a Reducing Agent. *Angew. Chem. Int. Ed. Engl.* **2010**, *49*, 6156–6159.
68. Wu, B.; Zheng, N.; Fu, G. Small Molecules Control the Formation of Pt Nanocrystals: A Key Role of Carbon Monoxide in the Synthesis of Pt Nanocubes. *Chem. Commun. (Camb).* **2011**, *47*, 1039–1041.
69. Brinson, B.E.; Lassiter, J.B.; Levin, C.S.; Bardhan, R.; Mirin, N.; Halas, N.J. Nanoshells Made Easy: Improving Au Layer Growth on Nanoparticle Surfaces. *Langmuir* **2008**, *24*, 14166–14171.
70. Rahman, M.T.; Krishnamurthy, P.G.; Parthiban, P.; Jain, A.; Park, C.P.; Kim, D.-P.; Khan, S.A. Dynamically Tunable Nanoparticle Engineering Enabled by Short Contact-Time Microfluidic Synthesis with a Reactive Gas. *RSC Adv.* **2013**, *3*, 2897–2900.
71. Dahl, J.A.; Maddux, B.L.S.; Hutchison, J.E. Toward Greener Nanosynthesis. *Chem. Rev.* **2007**, *107*, 2228–2269.
72. Dupont, J.; Scholten, J.D. On the Structural and Surface Properties of Transition-Metal Nanoparticles in Ionic Liquids. *Chem. Soc. Rev.* **2010**, *39*, 1780–1804.
73. Torimoto, T.; Tsuda, T.; Okazaki, K.; Kuwabata, S. New Frontiers in Materials Science Opened by Ionic Liquids. *Adv. Mater.* **2010**, *22*, 1196–1221.
74. Lazarus, L.L.; Yang, A.S.-J.; Chu, S.; Brutchey, R.L.; Malmstadt, N. Flow-Focused Synthesis of Monodisperse Gold Nanoparticles Using Ionic Liquids on a Microfluidic Platform. *Lab Chip* **2010**, *10*, 3377–3379.
75. Lazarus, L.L.; Riche, C.T.; Marin, B.C.; Gupta, M.; Malmstadt, N.; Brutchey, R.L. Two-Phase Micro Fl Uidic Droplet Flows of Ionic Liquids for the Synthesis of Gold and Silver Nanoparticles. *ACS Appl. Mater. Interfaces* **2012**, *4*, 3077–3083.
76. Gomez, L.; Sebastian, V.; Irusta, S.; Ibarra, A.; Arruebo, M.; Santamaria, J. Scaled-up Production of Plasmonic Nanoparticles Using Microfluidics: From Metal Precursors to Functionalized and Sterilized Nanoparticles. *Lab Chip* **2014**, *14*, 325–332.
77. Lohse, S.E.; Eller, J.R.; Sivapalan, S.T.; Plews, M.R.; Murphy, C.J. A Simple Milli-Fluidic Benchtop Reactor System for the High-Throughput Synthesis and Functionalization of Gold Nanoparticles with Different Sizes and Shapes. *ACS Nano* **2013**, *7*, 4135–4150.